U.PORTO

FEUP FACULDADE DE ENGENHARIA UNIVERSIDADE DO PORTO

MASTER IN ENVIRONMENTAL ENGINEERING 2022/2023

ASSESSMENT OF SOIL HEALTH IN THE VICINITY OF A GOLD/ANTIMONY MINE, MONTALTO MINE CASE STUDY

ANDRÉ FILIPE DA SILVA ALVES

Dissertation presented to obtain the degree of
Masters in Environmental Engineering

President of the Jury:
Adrián Manuel Tavares da Silva, Professor Associado do Departamento de Engenharia Química da Faculdade de Engenharia da Universidade do Porto

---

Supervisor:
António Carlos Pinheiro Fernandes, Professor Auxiliar Convidado, Departamento de Engenharia de Minas da Faculdade de Engenharia da Universidade do Porto

---

Co-Supervisor:
Maria Cristina da Costa Vila, Professor Associado, Departamento de Engenharia de Minas da Faculdade de Engenharia da Universidade do Porto

---

July 2023

Edited by:
FACULTY OF ENGINEERING OF THE UNIVERSITY OF PORTO
Rua Dr. Roberto Frias
4200-465 PORTO
Portugal
Tel. +351-22-508 1400
E-mail : feup@fe.up.pt
Website : http://www.fe.up.pt

Resumo

Este estudo teve como objetivo investigar a contaminação do solo nas proximidades da antiga Mina de Montalto, por meio de análise a amostras de solo. Os objetivos principais foram avaliar a qualidade do solo, explorando a presença de contaminantes nas amostras e seus possíveis impactos na população local e no meio ambiente da região.

Para atingir esses objetivos, um total de 21 amostras de solo foram colhidas em vários locais da área em estudo. Diferentes propriedades do solo foram medidas, nomeadamente: pH do solo, carbono orgânico total, humidade e textura do solo, potencial de geração ácida e análise química elementar por fluorescência de raios-x (FRX). A análise da distribuição do tamanho das partículas revelou uma composição predominantemente grosseira, indicando um risco aumentado de transporte de contaminantes. Em alguns dos locais, partículas maiores (cascalho) mostram a deposição de escombro. As medições de pH do solo indicaram condições ligeiramente ácidas a neutras (o valor mais baixo é 4,7 e o mais alto 7,3), o teor de carbono orgânico variou entre as amostras (0,7% a 5,0%). A análise FRX revelou uma concentração significativa de metais pesados, particularmente em arsénio, antimónio e chumbo, com concentrações até os 747 ppm, 2017 ppm e 214 ppm, respetivamente. O potencial de geração de ácido observado levantou preocupações sobre a possibilidade de drenagem ácida mineira em conjunto com metais pesados para certas áreas em particular, como as instalações da mina, que atualmente são usadas para agricultura e habitação.

As amostras mais contaminadas foram colhidas nos arredores da mina e apresentaram uma elevada concentração de metais pesados (PS_10 e PS_15). Outras amostras contaminadas foram também colhidas dentro das antigas instalações da mina (PS_06 a PS_11). As amostras indicaram uma clara influência das atividades de mineração na qualidade do solo, com níveis elevados de contaminantes que representam riscos potenciais ao meio ambiente e à população. Algumas amostras apresentaram níveis moderados de contaminação (PS_04, PS_05, PS_12 e PS_20). Essas amostras podem apresentar valores normais de pH e COT, indicando condições de solo relativamente saudáveis. No entanto, também mostram níveis baixos de concentrações de metais pesados em comparação com as amostras contaminadas e de referência, sugerindo um menor impacto de contaminação nessas áreas. Por outro lado, amostras colhidas em áreas localizadas na margem do rio oposta à das antigas instalações da mina, apresentaram concentrações de metais pesados comparativamente menores ou nulas (PS_01 a PS_03 e PS_18) sendo consideradas não contaminadas. Estas amostras, respeitam os limites recomendados pela Agência Portuguesa do Ambiente, não foram significativamente afetadas pela mina e demonstraram um impacto

comparativamente menor na qualidade do solo. Além disso, amostras de referência retiradas de locais mais distantes da mina apresentaram baixos níveis de contaminação (116 mg/kg de antimónio e 35 mg/kg de arsénio) e serviram de referência para estabelecer um padrão de qualidade do solo para a região (PS_16 e PS_17).

Em conclusão, este estudo forneceu informações valiosas sobre a composição e o estado de contaminação da área de estudo. Os resultados enfatizam a urgência de implementar ações de remediação para lidar com a contaminação por metais pesados, prevenir a drenagem ácida mineira e proteger a saúde humana e o meio ambiente.

Palavras-chave: Antimónio; Arsénio; Contaminante; Escombro; Rejeitos; Mina de Au/Sb; Qualidade do solo.

Abstract

The present study aimed to investigate the soil contamination in the vicinity of the inactive mine “Montalto Mine”, through a comprehensive analysis of soil samples. The primary objectives of this study were to assess the soil quality by exploring the potential presence of contaminants in the samples and trace possible impacts on the region's environment, regarding the local population health.

To achieve these objectives, a total of 21 soil samples were collected from various locations across the study area. Different soil properties were measured, namely: soil pH, total organic carbon, soil moisture and texture, net acid generation, and elemental chemical composition by X-ray fluorescence (XRF). Particle size distribution analysis revealed a predominantly coarse composition, indicating an increased risk of contaminant mobility. At some of the sites, larger particles (gravel) display the deposition of waste rock. Soil pH measurements indicated slightly acidic to neutral conditions (lowest value is 4.7, highest 7.3), and organic carbon content varied across the samples (0.7% to 5.0%). XRF analysis unveiled the concentration of heavy metals, with certain samples displaying significant contamination, particularly arsenic, antimony, and lead, with concentrations up to 747 ppm, 2017 ppm and 214 ppm, respectively. The observed acid generation potential raised concerns about the possibility of acid mine drainage in specific areas, such as the mine facilities currently used for farming and housing.

The most heavily contaminated samples were obtained from the periphery of the mine facilities and showed high concentrations of heavy metals (PS_10 and PS_15). Some of the contaminated samples are the ones located inside the mine facilities (PS_06 to PS_11). These samples indicated a clear influence of mining activities on the soil quality, with high levels of contaminants posing potential risks to the surrounding environment and population. Some samples demonstrated moderated levels of contamination (PS_04, PS_05, PS_12 and PS_20). These samples might display normal values of pH and TOC, indicating relatively healthy soil conditions. However, also show lower levels of heavy metal concentrations compared to the highly contaminated and reference samples, suggesting a minor contamination impact in these areas. On the other hand, samples collected from areas located on the other side of the river showed relatively lower heavy metal concentration (PS_01 to PS_03, and PS_18) and are considered not contaminated. These samples, respecting the limits recommended by the Portuguese Environmental Agency, were not significantly affected by the mine and demonstrated a comparatively lower impact on soil quality. Additionally, reference samples taken from locations further away from the mine exhibited minimal contamination (116 mg/kg for antimony

and 35 mg/kg for arsenic) and served as benchmarks for establishing a standard soil quality for the region (PS_16 and PS_17).

In conclusion, this study provided valuable insights into the composition and contamination status of the study area. The results emphasize the urgency of implementing remediation actions to address heavy metal contamination, prevent acid mine drainage, and protect human health and the environment.

Keywords: Antimony; Arsenic; Contaminant; Waste rock; Tailings; Au/Sb Mine; Soil health

Acknowledgements

I would like to express my heartfelt gratitude to Professor António Fernandes for his unwavering availability, exceptional guidance, invaluable support, shared knowledge, unwavering dedication, and remarkable companionship throughout this semester and the completion of this work. It is with great conviction that I believe these combined efforts have led to an exceptional outcome in this work.

To Professor Cristina Vila for also sharing her expertise, and feedback which offered valuable suggestions for improvement, that enhance the quality of this thesis.

I extend my heartfelt gratitude to FEUP for granting me the opportunity to undertake this work and providing access to their laboratories. Over the past two remarkable years, FEUP has not only facilitated my learning but also fostered my personal growth, enabling me to evolve as an individual.

To my colleagues, who I can call friends, who have walked this path alongside me, transforming this journey into a remarkable and cherished experience. Your companionship, support, and the friendships we have forged are something I will cherish forever. Your presence and the memories are a treasure that has truly enriched this chapter of my life.

I want to express my heartfelt gratitude to my friends who may not have walked this path with me but have consistently shown their unwavering love and support. Your presence and encouragement have meant the world to me, and I deeply appreciate the bond we share. Thank you for always being there for me.

I would like to extend my sincerest gratitude to my beloved family, who have not only granted me the opportunity to pursue this study but have also been unwavering in their support and belief in me. Their unconditional love and unwavering support have served as the catalyst for my achievements, and I wholeheartedly dedicate all of my accomplishments to them.

This work is a result of the project “Soil health surrounding former mining areas: characterization, risk analysis, and intervention”, with the reference NORTE-01-0145-FEDER-000056, supported by Norte Portugal Regional Operational Programme (NORTE 2020), under the PORTUGAL 2020 Partnership Agreement, through the European Regional Development Fund (ERDF).

This work was financially supported by: Base Funding - UIDB/04028/2020 and Programmatic Funding - UIDP/04028/2020 of the Research Center for Natural Resources and Environment – CERENA - funded by national funds through the FCT/MCTES (PIDDAC).

Contents

List of Figures

List of Tables

Acronyms and Symbols

AMD - Acid Mine Drainage
APA - Portuguese Environmental Agency
CBD - Baixo-Douro Consortium
EMS - Environmental Management System
EGDI - European Geological Data Infrastructure
IPB - Iberian Pyrite Belt
NAG - Net Acid Generating
NAF - Non-Acid Forming
OM - Organic Matter
PSD - Particle size determination
SIORMINP - Portuguese Mineral Resources and Occurrences Information System
LNEG - National Laboratory of Energy and Geology
TOC - Total Organic Carbon
USDA - United States Department of Agriculture
XRF - X-Ray Fluorescence

1 Introduction

1.1- Open Remarks

Throughout human civilization, mining has played a key role in catalysing innovation, particularly during the industrial revolution. This important industry has contributed to numerous sectors' development and fostered a constant economic flow in various regions, thereby transforming and shaping society (Clifford et al., 2018). By providing essential materials, mining has fuelled technological advancements and enabled the growth of industries. The economic significance of mining cannot be established, as it has supported economic prosperity, job opportunities, and societal advancements. Portugal possesses a noteworthy potential in terms of mineral resources, and this potential can play a crucial role in revitalizing the economy (Leite and Silva, 2013).

The mining industry is accompanied by the significant generation of waste during mineral extraction and processing. Among these waste materials are tailings and overburden, also known as waste rock. Mine tailings refer to crushed rock that remains after valuable metal-bearing minerals have been extracted through separation techniques (Pacheco-Torgal, 2015). However, the sheer quantity of these waste materials poses a significant threat to the local population and the surrounding environment. In many cases, the disposal of mining waste involves the practice of dumping at designated sites, which can result in soil degradation and water pollution. Additionally, the deposition covers land that could otherwise be utilized for various purposes (Lazorenko et al., 2021).

At the local level, the outcomes of mining are often adverse. Additionally, there is a link to the social and economic implications of mining activities, particularly for the people who live in mining regions and are dependent on agriculture. Abandoned mining sites are frequently associated with pollution, population decline due to out-migration (Svobodova et al., 2022), inadequate infrastructure, economic contraction, and a lack of diversification into other economic activities. While this narrative is not universally true, it resonates due to shared experiences (EDM & DGEG, 2011). Overall, there is a need to take a comprehensive approach to mining, considering both the environmental and social impacts, in order to develop sustainable mining practices that minimize harm to the environment and local communities.

The current work is a component of the “Soil health surrounding former mining areas: characterization, risk analysis, and intervention” project, representing an essential part of environmental sciences. Within the scope of the project, it is intended to characterize the vicinity

of abandoned mines in the Northern Region of Portugal, and also to trace environmental impacts. This soil characterization offers a broader perspective beyond mining areas, encompassing the environmental ecosystem of Portugal.

Valongo Anticline, located in the north of Portugal, stands has a geological formation known for its mineral wealth. Hosting a range of valuable metals, including gold and antimony, it pertains to an area of interest for mining activities. One example is the Montalto Mine, located in the municipality of Gondomar, Porto district. The Montalto Mine operated from 1863 to 1906, contributing to the exploration of great quantities of gold and antimony. (Couto, 1993) (Silva, 2017)

The Montalto mine is the study area for the present dissertation. It is a region with a small population, most of whom work in agriculture and livestock production. The surrounding landscape is characterized by extensive green zones and the Sousa River that flow into the Douro River.

1.2- Goals

The main goal of this dissertation is to identify and assess the primary environmental impacts on soil caused by mining activity in the vicinity of the former Montalto mine.

The specific objectives will be to determine and analyse soil properties using samples collected in the field and ascertain which are the contaminated zones in the vicinity of Montalto Mine. The dissertation work will consist of a comprehensive review of relevant literature, analysis of existing data, soil sample collection, measurement of key environmental parameters, and interpretation of obtained results. By integrating these elements, this study aims to provide a comprehensive understanding of the impact of mining activity on the surrounding soil environment at the Montalto mine.

1.3- Project Plan

The research presented in this study was conducted as part of the academic program at the Faculty of Engineering of the University of Porto, with a significant focus on practical application. The laboratories from the Mining Engineering Department were used to conduct the necessary experiments.

The methodology for studying soil quality in mining areas typically involved field sampling and laboratory analysis of various physical, chemical, and biological properties of the soil. The results are then compared to established guidelines. In this sense, the following experiments were conducted: particle size analysis, net acid generation potential, total organic carbon content, elemental chemical analysis by X-ray fluorescence, and soil pH, focusing on the presence and concentration of heavy metals, particularly those commonly associated with gold/antimony mining.

The research for this project spanned 13 weeks, starting from the beginning of February till the end of May. The first few weeks were dedicated to an extensive literature review and two field trips to obtain the soil samples for analysis. Subsequently, several weeks were spent in the laboratory carrying out various procedures, such as sample preparation (e.g., separation, drying, and storage), and determining the mentioned soil properties.

1.4- Structure

The structure of this dissertation is organized as follows:

Chapter 1: This chapter serves as an introduction to the study, providing the framework, motivation, and context for the research. It outlines the primary objectives and presents an overview of the document's structure.

Chapter 2: This section offers an introduction to the mining industry, exploring its historical significance and contemporary relevance. Most important, approaches the environmental impacts associated with mining activities and highlights the industry's relevance today. Additionally, it delves into specific themes that depict the current state of the industry, focusing on the Valongo Anticline, Montalto mine, and its surrounding area.

Chapter 3: In this chapter is demonstrated how the research was conducted, and the step-by-step process from the sampling to the determination of soil properties. It provides the investigation's methodology, detailing the specific methods employed, their underlying principles, and the rationale behind their selection.

Chapter 4: Focuses on the presentation, analysis, and interpretation of the conducted work in this study, providing valuable insights into the collected data. The obtained results are then thoroughly examined and discussed by category, allowing for a comprehensive assessment of their consistency and relevance. There’s also a global analysis, that explores the interpretations

of the results, aiming to characterize the soils and determine which samples are contaminated. Furthermore, there will be a section dedicated to mitigation measures and further works.

Chapter 5: The final chapter contains the conclusions derived from this study, whether or not the objectives were accomplished, along with suggestions for future research to ensure its continued progress.

2 State of the art

2.1- Mining Industry

2.1.1- Mining Industry and the Environment

There is a growing recognition of the importance of the industry's sustainability and social responsibility. This concern has gained significant attention from countries and various industries, with particular emphasis on the mining sector. In the mining industry, one noticeable consequence is the escalating requirement for companies to substantiate their purpose and demonstrate their performance, not only through public transparency in social aspects but also by providing pertinent environmental information (Jenkins and Yakovleva, 2006). As such, implementing an Environmental Management System (EMS) is crucial for effectively managing and mitigating environmental impacts. An EMS serves as a comprehensive framework that enables organizations to identify potential environmental impacts, enhance their environmental performance, and ensure compliance with relevant regulations and standards, often based on ISO 14001 guidelines. Adopting such a system in mining ensures the adoption and adherence to corporate environmental policies (Hilson and Nayee, 2002). For example, within the mining supply chain, various practices can be implemented to support environmental sustainability. Some suggestions include implementing Green Information Technology to reduce energy consumption, establishing Strategic Supplier Partnerships to communicate and achieve environmental goals with suppliers, integrating Operations and Logistics to optimize the efficient organization of raw materials, establishing Internal Environmental Management systems to foster continuous employee training and adherence to environmental practices, conducting audits, and reporting. Additionally, embracing Eco-Innovation processes that reduce environmental risks and incorporating End-of-Life practices, such as recycling and waste recovery, are essential (Kusi-Sarpong et al., 2015).

Despite the various potential implementations and waste management approaches available, in 2020, the total waste generated in the European Union amounted to 2135 million tonnes. Mining and quarrying rank as the second largest waste-generating activity, contributing to 23.4% of the total waste, of which 64% constitutes mineral waste (Eurostat, 2023). In 2001, in Portugal, the mining and quarrying sector contributed to a significant portion of industrial waste, amounting to 17 million tons, which represents 58% of the total generated. (Grangeia et al., 2011). Nowadays, Portugal generates a lot less waste from mining activity. However, there remains a concerning issue of abandoned mines throughout the country.

2.1.2- Deposition of waste by the mining industry

Mine waste and mine tailings are two distinct types of waste materials from mining activities. Mine waste primarily refers to the bedrock that has been excavated from the mine pit but lacks

economically valuable metals (Araujo et al., 2022). This waste material includes overburden, which can serve various purposes after reprocessing, such as a construction aggregate for buildings and roads (Sims et al., 2019). To deposit mine waste, several methods can be employed depending on factors such as the type of waste, local regulations, and available infrastructure. Historically, mine waste was often deposited in open-pit heaps, dumps, or uncontrolled mine cavities, leading to risks of erosion, leaching, and contamination of surrounding ecosystems (EDM and DGEG, 2011). Tailings are a waste product of typically no financial value, so are usually stored in the most cost-effective manner to meet regulations and site-specific factors. The constant growth in waste volume poses one of the problems of tailings storage. Technological advancements enabling the exploration of lower-grade ores further contribute to this increase. Compounded with stricter environmental regulations, the mining industry faces additional requirements, making the establishment of effective tailings storage measures more challenging(Dixon-Hardy and Engels, 2007). Tailings disposal methods encompass a range of practices. One approach involves backfilling these tailings into pre-existing underground mining voids or cavities. However, the prevalent method involves constructing dams using mine waste materials to confine and contain the tailings. These engineered structures serve as storage facilities, ensuring the retention and management of potentially hazardous tailings (Schoenberger, 2016).

The key principles of a tailings storage facility involve ensuring its long-term stability, minimal environmental impact, and the ability to be rehabilitated after closure (Dixon-Hardy and Engels, 2007). This line of thinking, together with early planning and strategy, helps implement a successful tailings storage facility that prioritizes the protection of the surrounding environment and communities. In recent times, increasing attention has been given to the potential for reusing these materials, leading to the emergence of recycling practices aimed at transforming them into valuable resources. This development has extended into diverse sectors, including mining, construction, building, chemistry, energy, and even environmental rehabilitation, opening up new ways for their utilization as valuable resources (Yilmaz et al., 2023). While there may be a lack of specific legislation and standardized practices in this field, the utilization of mining wastes in alternative applications has shown promising outcomes. Moreover, reusing tailings can contribute to the preservation of soil's inherent properties, maintaining its original characteristics and minimizing disruptions to ecosystems. By reducing waste volume and providing sustainable raw materials, the reuse of mine tailings has considerable environmental and resource conservation advantages (Segui et al., 2023).

2.1.3- Case studies

Portugal possesses a rich array of mineral resources, a testament to its geological diversity and unique geological formations. In the northern and central regions, there are deposits of metallic ores such as tin, tungsten, gold, silver, zinc, lead, lithium, and uranium, often associated with Paleozoic and older metamorphic and igneous rocks. In the southern region, specifically in the Iberian Pyrite Belt (IPB), there are significant occurrences of copper-zinc massive sulfides. Outside the continent, Azores and Madeira, have been the subject of scientific research on iron-manganese nodules and hot springs containing sulfides rich in metals (Leite and Silva, 2013). Notable mines in Portugal include Panasqueira one of the world's leading producers of tungsten concentrates outside of China, and Neves-Corvo one of the largest producers of mined copper within the European Union, both deposits that have continued operations even during periods of low metal prices (Julio, 2008; Real, 2016).

According to the Portuguese Mineral Resources and Occurrences Information System (Sistema de Informação de Ocorrências e Recursos Minerais Portugueses - SIORMINP), which has been developed since 1997 to include all known mineral deposits in the country, 2002, the system identified a total of 2,164 mineral deposits across the entire continental territory of Portugal. As of 2020, the number of registrations in SIORMINP had increased to 2,292, and it is projected that in the coming years, the system will encompass approximately 2,500 registrations (Inverno et al., 2020).

In Portugal, there are notable instances of environmental contamination caused by mining activities. One such example is the Panasqueira mine (Barroca Grande), mining activities contribute to elevated metal/metalloid levels in tailings, soils, and water. Tailings and open impoundment materials disperse through wind, have been showed impacting rhizosphere soils downstream. Road dust analysis indicates significant wind dispersion of As, Cd, Cu, and Zn. Also, vegetables grown in the area are contaminated, with As, Cd, and Pb concentrations above the maximum permitted level, which could pose a potential health risk to residents by consuming products sourced from contaminated areas. As such, soils in S. Francisco de Assis village exceed As reference values by 20 times (Candeias et al., 2014).

Exploring the environmental consequences of a Pb-Zn abandoned mine in Aveiro district, a study analysing samples from the mine site investigated the environmental impacts downstream (Ferreira da Silva et al., 2009). The results revealed a decreasing metal gradient in stream sediment samples along the Coval da Mó and Fílvida streams, indicating contamination in the old

mining area. The assessment based on established guidelines revealed the presence of elevated toxicity in the Coval da Mó stream.

With the recent increase in metal prices, Portugal has attracted prospecting enterprises to explore gold, silver, tin, tungsten, base metals, lithium, and iron ores. (Leite and Silva, 2013). In 2017, Portugal made significant strides in the mining sector, emerging as the fifth-largest producer of lithium worldwide, representing 1.2% of global production. Additionally, the country ranked seventh in tungsten production, accounting for 0.9% of the world's output. These accomplishments played a pivotal role in fostering Portugal's economic expansion, with a noteworthy 3.5% increase in real gross domestic product during the same year. The mining industry's contributions not only bolstered Portugal's position in the global market but also stimulated domestic economic growth, reinforcing the sector's importance to the nation's overall development (Goclawska and USGS, 2022).

2.1.4- Environmental Impacts

Mining is an industry that has been in continuous evolution, leading to the development of innovative methods and technologies for more efficient ore extraction and processing. However, many of these innovations failed to effectively address environmental pollution and its harmful effects on human health. The regulation of the mining industry is often characterized by a more responsive approach after problems arise, rather than a proactive one in taking preventive measures in advance and enforcing the protection of the environment and the population surrounding it (EDM and DGEG, 2011).

Mining operations can have significant environmental impacts, particularly through mine waste and tailings that are usually associated with the dehydration of water bodies, soil erosion, and damage to infrastructures (Mencho, 2022). Environmental impact arises from mineral leaching and mine acid drainage, whereby oxygen and water intrusion into tailings triggers chemical changes, leading to the production of acidic water containing dissolved heavy metals (Lopes, 2022; Moreno and Neretnieks, 2006). This process occurs through molecular diffusion and advection, contributing to the migration of contaminants. Moreover, the presence of precipitation is a significant driver for the movement of heavy metals from mine tailings into surrounding areas (Desogus et al., 2013), while the evaporation of porewater in tailings regulates the transfer of mobile metals to overlying soils (Zhang et al., 2016).

Depending on the geological properties of the mining area, common toxic metals found in mine tailings dumps include lead, zinc, copper, nickel, manganese, and arsenic. A study conducted on the Lead-Zinc mine of Kabwe, Zambia has revealed the creation of a regional environmental anomaly as a result of mine tailings (Munanku et al., 2023). This anomaly poses a significant health risk, particularly affecting livestock and vulnerable population such as children. Additionally, the safety and stability of mine tailings dumps have become a prominent concern, with potential implications for geotechnical stability and overall safety.

Mining activities give rise to several negative effects, including the destruction of ecological integrity, loss of vegetation cover, food scarcity, changes in land use, and water pollution (Worlanyo and Jiangfeng, 2021). The conversion of natural ecosystems to other land uses, as a result of mining activities, can lead to the loss of species, changes in ecosystem composition, habitat fragmentation, and increased carbon emissions even beyond their lease boundaries, (Seki et al., 2022). Another example of significant environmental and health impacts has been shown during activities in a gold mine in the Kenyasi-Ahafo region of Ghana. (Addo et al., 2023). Air and noise pollution is attributed to the emission of dust, particles, and chemicals like carbon, sulfur, and arsenic but also from the explosive blasting of rocks. Water contamination is due to the presence of cyanide, arsenic, and other suspended particles. Also, the use of machinery, harmful chemicals, and the construction of tailings dams in open-pit mining have caused land degradation. All of these factors had direct and indirect major human health consequences, with a high prevalence of diseases such as malaria, cough or cold, and skin disorders among individuals living in the mining areas.

Various parameters can be measured to assess the environmental impact of mining activities, such as soil pH, total organic carbon content, net acid generation potential, and particle size distribution (Hu et al., 2020; Kundu et al., 2017; Loveland, 2003). These parameters offer valuable insights into the soil's acidity levels, propensity for acid generation, and organic matter composition. Moreover, analysing particle size distribution allows us to comprehend the soil's physical characteristics, influencing its capacity to retain or release contaminants. It is important to note that in general, mining exploitation, especially the deposition of waste rock or tailings can alter the soil's particle size distribution. In conjunction with these parameters, X-Ray Fluorescence (XRF) analysis aids in identifying the specific contaminants affecting the Montalto mine area. By comprehensively examining these factors, the aim is to obtain a general understanding of the environmental implications associated with mining activities in the studied region.

2.2- Valongo Anticline

The Valongo Anticline is situated in the Central Iberian Zone, 18 km east of Porto (Carvalho et al., 2013). Extending from Vila do Conde to the southern side of the Douro River, this strip spans approximately 90 km according to mining records. Within this area, besides the Sb-Au deposits, there exist additional mineralizations of Pb-Zn-Ag and W-Sn. The underlying rock formations, dating back to the Carboniferous periods, exhibit diverse layers from different periods (Couto, 2013), which consist of conglomerates, quartzites, and schists. The normal flank of the anticline, along the Banjas mountain, Santa Justa, Pias, and Santa Iria, were known for their gold deposits, while the antimony mining, usually associated with gold extraction, was primarily concentrated on the reverse flank (Couto, 1993). Figure 1 exhibits a map with Valongo Mineral Belt extension.

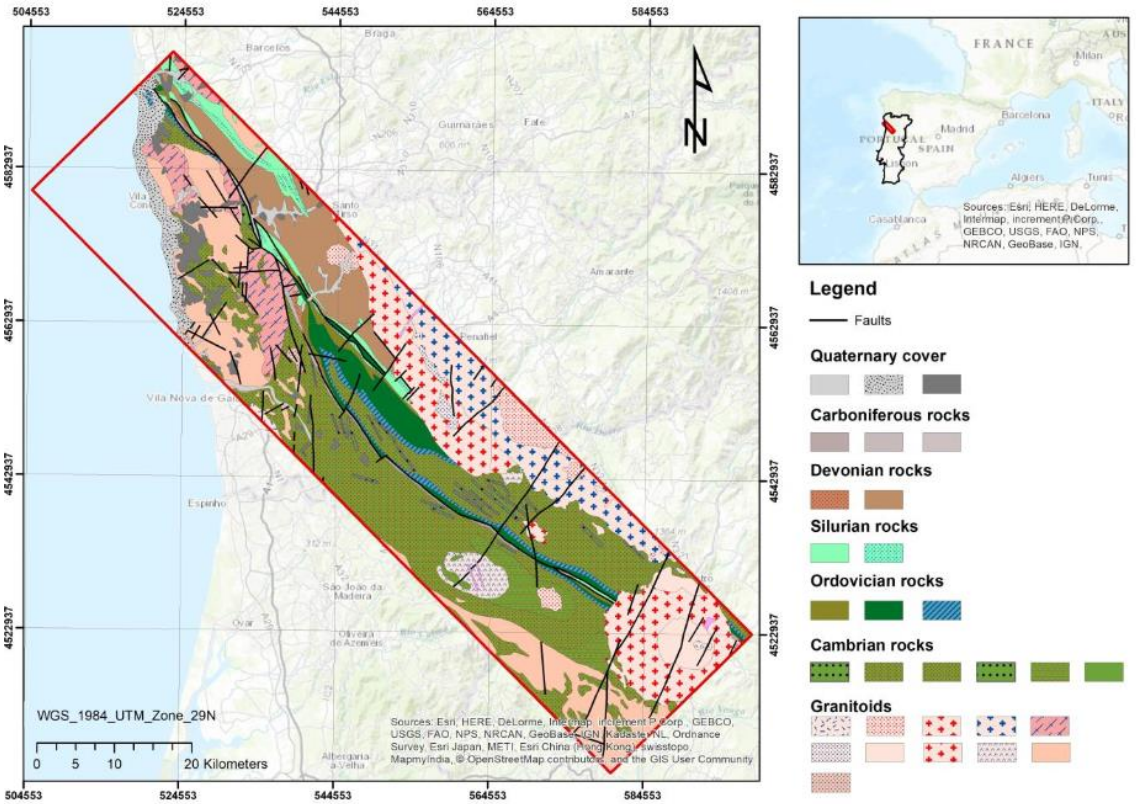

Figure 1 - Valongo Mineral Belt, extracted from (Fiúza et al., 2023)

The gold in this region has attracted human interest for a long time. The Iberian Peninsula has been mined by Roman settlers with simple methods of sieving (Fernández-Lozano et al., 2019). During the exploration of archaeological remains, it was discovered that the mining aqueduct exhibited typical Roman characteristics and was closely associated with the waste rock piles in the region. These findings provide strong evidence of the Romans' engagement in ore treatment and their extensive mining activities. The Santa Justa, Pias, Santa Iria, and Banjas mountain ranges, part of the Valongo Anticline, are known for their rich gold deposits and were particularly

favoured by the Romans for exploration and extraction purposes (Lima et al., 2015). There are also references to mining works from that period in the Medas and Covelo region, an area that was intensively worked for antimony (with associated gold) in the last centuries. It is known that they did not extract antimony (which was left in the waste heaps) as they were unfamiliar with its treatment. According to Couto, 1993, mining may have started even before the Roman era, pointing to the proximity of mining works to the coast. Some of these works, due to their dimensions and extent, demonstrate the importance of mining activity during this era (Couto, 1993).

The discovery of antimony and gold deposits in the region dates back to 1807 with Vale de Achas and Ribeiro da Igreja. Active mining operations began in 1858, followed by the opening of the Tapada and Ribeiro da Serra mines in 1880. The Montalto mine, established in 1881, became one of the region's most productive mines, reaching the peak of exploitation in the 1870s-1890s exporting thousands of tons of antimonite concentrate annually (Couto, 1993). The activities were concentrated within a 5 km strip between Covelo and Alto do Sobrido. Antimony production declined in the early 20th century, with some mines continuing operations until the 1940s. By 1971, there were no active, producing deposits. In 1988, Baixo-Douro Consortium (CBD) carried out prospecting and geological exploration, reopening the Banjas and Moirama mines in 1990 for research purposes. (Couto, 1993).

In the north of Portugal, Sb, Pb–Sb, and Sb–Au-quartz veins are common. These veins contain minerals such as berthierite, stibnite, arsenopyrite, and pyrite, with native antimony and gold precipitating later. The ore mineral compositions indicate a common source for the veins (Neiva et al., 2008). It also observed a substitution of Sb for As in arsenopyrite, with fluid cooling identified as the main cause of ore precipitation. These findings highlight the environmental implications associated with the presence of these minerals and the geological processes involved in their formation.

Acidity in soils plays a significant role in enhancing the adsorption of arsenic and antimony, especially in their anionic forms. Soils contaminated by antimony and arsenic from old mining activities show elevated levels of heavy metals, which are readily available. Certain elements, such as Cr, Cu, Ni, Pb, and Zn, tend to associate more with organic matter, while arsenic demonstrates a stronger affinity for adsorption by iron, and antimony by manganese (Carvalho et al., 2012). The behaviour of As and Sb in stream sediments is similar, predominantly retained in the residual fraction and associated with the clay minerals. The pH values of stream sediments favour adsorption into clays and as such explain the elevated concentrations in this compartment.

Waters from abandoned Sb-Au and As-Au mining areas in Valongo are contaminated with various elements, being declared not appropriate for human consumption (Carvalho et al., 2014).

Fiúza et al., 2023, verified the environmental impact of an ancient antimony mine near Montalto and concluded that although not visibly apparent, the site has undergone geomorphological alterations and composition changes in environmental compartments due to open-pit storage of mine wastes, although it's not visible as usually in abandoned mines. Acid mine drainage is not observed, but soil analysis reveals the presence of acidic soil with elevated levels of Sb and As, exceeding regulatory thresholds (Fiúza et al., 2023). If there are no changes to the current conditions, the closure of the mines since the late nineteenth century has contributed to the stability of elements associated with mineral phases. However, it is important to note that median values of arsenic and antimony in Montalto soils surpass Italian and Dutch regulatory limits. (Carvalho et al., 2012). These levels of concentration pose potential health risks and indicate the distinct environmental impact of the mine compared to the background levels. The concealed nature of waste storage sites and minimal ruins further emphasize the challenge of detecting and managing the environmental problems it arises.

2.3- Case study

Mining activity in Montalto began in 1863, initially exploring only antimony. It was only from 1881 onwards that the mine began to explore for gold as well. The provisional concession for the Montalto mine was obtained in 1864. The discovery of gold in the mine aroused the interest of industrial miners in the district of Porto in 1887. The exploration of the mine lasted until 1906 when it ended its activities. The interruption of exploration was due to competition from Asian countries, which caused a crisis in European markets and led to the stoppage of Portuguese mines. In addition, Companhia das Minas de Montalto faced difficulties due to a lack of capital and adequate management, which significantly reduced the mine's productivity (Silva, 2017).

At the Montalto mine, mainly antimony and gold were extracted. The presence of gold in quartz can vary between 1 and 70 g/t, frequently accompanied by Au in ratios ranging from 44 to 460 g/t. (Couto, 1993). The mine extracted a total of 6763 tonnes of antimonite from the beginning of exploration in 1864 until 1883 (Carvalho, 1970) Ore treatment processes included mechanical preparation, where the ore was put through various sorting machines to separate the antimony from the gangue and other unwanted materials. The ore was placed in sieves and trommels of varied sizes for proper antimony selection and analysis (Silva, 2017). As for the deposition of waste from the exploitation, the waste was probably deposited in heaps and tailings basins, which

were commonly used at the time. These places were designated to store the discarded materials during the process of extracting and treating the ore (EDM and DGEG, 2011).

There are environmental and health concerns around the Montalto Mine, due to the proximity to the Sousa River, the practice of agriculture and livestock, and the green landscape surrounded by mountains and forests. One primary concern might be the flooded galleries in the abandoned mines, particularly those affected with higher concentrations of various contaminants such as Zn, Ni, Cd, Pb, Sb, and As. These elevated levels of heavy metals and metalloids can pose a threat to the quality of the river water, potentially impacting aquatic life and ecosystems (Fiúza et al., 2023). The same can be said when we discuss the practice of agriculture in the Montalto region. Previous soil analysis indicates the presence of heavy metals and metalloids, including As and Sb, in concentrations that exceed regulatory thresholds (Lopes, 2022). Such contamination suggests that the soil may not be suitable for agriculture due to potential toxicity and low organic matter content. Cultivating crops or raising livestock in these areas could lead to the accumulation of harmful substances in the food chain, posing risks to human health (Carvalho et al., 2012).

Overall, the environmental impacts observed in the Montalto region raise concerns about the proximity to the Sousa River, the practice of agriculture, livestock rearing, and even some leisure activities. It is important to assess and mitigate these impacts to ensure the protection of ecosystems, human health, and sustainable land use practices in the area.

3 Methodology

The sampling process began by collecting 21 samples, 2 kg of soil for each, which were carefully placed in individual bags and stored at the FEUP facilities. The samples were subdivided using a Sample Divider, Figure 2. Initially, a 50/50 split was performed, where one portion remained with the original moisture, while the other portion was dried at 105ºC for 24 hours. During the drying process, the soil moisture was determined by weight loss.

Figure 2 – Example of Sample Divider used

As demonstrated on the right side of Figure 3, 50% of the sample was air-dried and sieved at 2 mm, and the particles with a diameter < 2mm were used for the determination of soil pH.

The dried samples (at 105 °C) were further subdivided into a 25% and 75% split. The 75% was used for the determination of particle size distribution. The 25% fraction contained was separated (through sieving) into > 2 mm and < 2 mm. Both were separately ground to < 75 µm using a ring mill and then stored.

The net acid generation (NAG) tests and XRF analysis were conducted in the crushed samples for both of the particle size classes. However, it is worth noting that a few samples from the > 2 mm fraction contained a minimal amount of gravel, resulting in empty values for both tests. The total organic carbon (TOC) determination was performed only on the grounded subsamples that initially had a particle size > 2 mm

Chapter 3 - Methodology

The determined properties discussed in this study were examined in the context of the impacts resulting from the deposition of tailings and waste rock. It is essential to consider these influences when interpreting the results. The presence of tailings and waste rock can introduce various elements and compounds into the soil, potentially affecting soil chemistry, nutrient availability, and overall soil fertility. The composition of these materials can include heavy metals, sulfides, and other potentially toxic substances, which may have detrimental effects on soil quality.

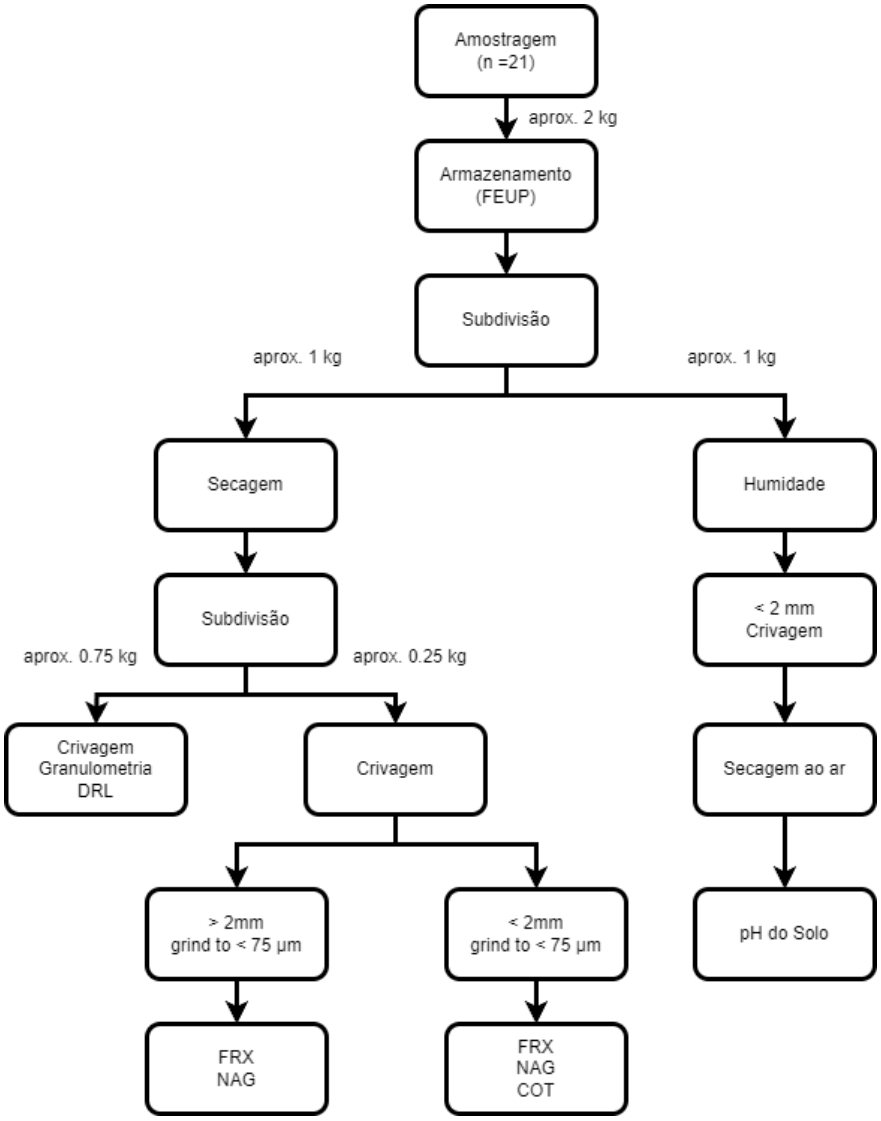

Figure 3 – Diagram of the methodology used in this study

3.1- Sampling

The collection of soil samples spanned two full days, a total of 21 samples were gathered. The selection of sampling locations was based on the previous work of Lopes, 2022. One significant area of interest was the facilities of the Montalto mine, which are currently used for farming and housing. In this vicinity, eight samples were collected, primarily from agricultural soil (PS_04,

PS_07, PS_08, PS_09, PS_10, PS_11, PS_19, PS_ 20 e PS_21), one other sample was taken in this land next to a platform that possibly showed tailings (PS_06). Three samples were taken from an area where tailings were visible, and that had previously been highlighted in Lopes' work (Lopes, 2022). (PS_13, PS_14 e PS_15), one sample was taken from a close-by forest area (PS_12). Additionally, two samples were obtained from a park situated next to the Sousa River, known as a leisure spot for the community (PS_01, PS_02). Another two samples were collected from a hill near residential units and a children's playground. (PS_03, PS_18), where according to the local population there's the deposition of waste rock. One sample was gathered from agricultural land (PS_04) and another from an area near a riverside location (PS_05). Furthermore, a pair of samples were obtained above the mine's influence line, serving as reference points for analysing soil unaffected by mine contamination (PS_16, PS_17). Figure 4 shows a map that pinpoints all the described locations and Appendix I contain the details for the collected sites.

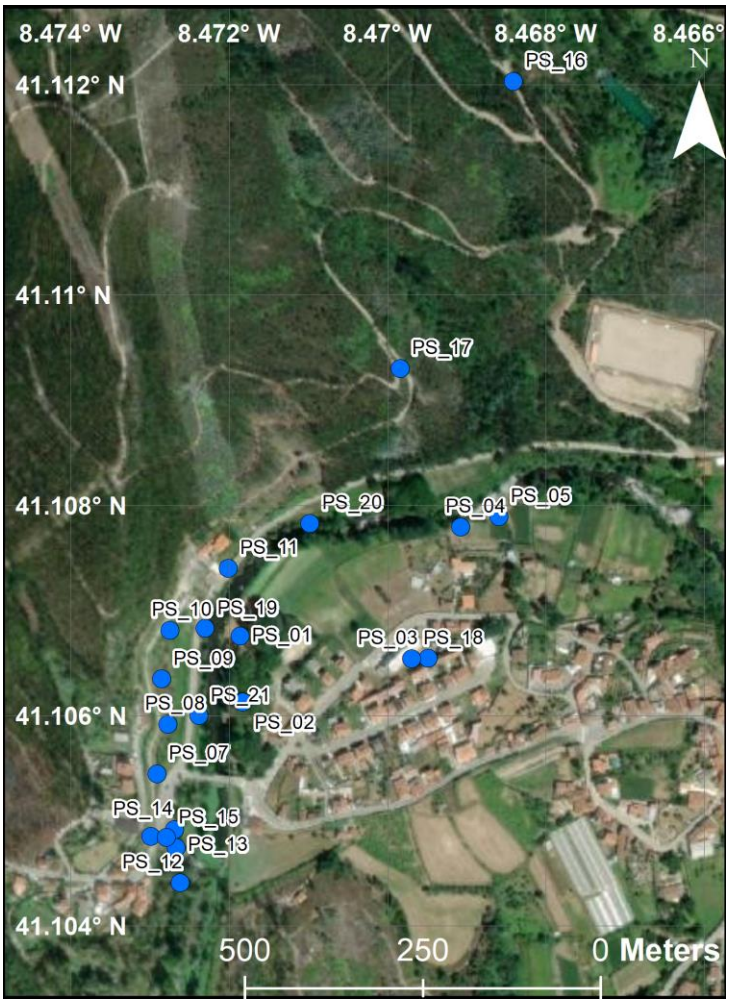

Figure 4 – Map of samples collected near Montalto mine, Covelo, Gondomar.

At each sampling site, the first 5 cm of soil was removed, then it was excavated to a depth of approximately 15 cm (Figure 5) and placed in individual plastic bags, clearly labelled with their respective sample names. They were then transported to the laboratory and stored. Then the samples were submitted to the procedures depicted in Figure 3.

Figure 5 – Soil before (A) and after (B) sampling

Based on a review of the current literature, it is expected that some of the collected samples, particularly those closest to the mine, are contaminated. This result is of great interest as it could have implications for the surrounding ecosystem and potential risks to human health (Lopes, 2022).

3.2- Experimental Methods

3.2.1- Moisture

Soil moisture is the amount of water held in soil pore spaces, expressed in terms of weight or volume. The availability of water to plants is influenced by soil tension or suction, and not all water in the soil is available for crops. Optimal soil moisture levels, which fall between field capacity and permanent wilting point, are necessary for proper aeration, nutrient availability, and biological activity, ultimately leading to higher crop yields (Prasadini and Mohan, 2019).

Water content can be easily determined by gravimetric or volumetric methods. This measurement involves initially weighing a soil sample in its moist state, followed by a drying period subjecting it to 105°C in an oven for around 24 hours. After, the soil sample is weighed again to obtain its dry weight. The difference between the wet weight and dry weight signifies the amount of water present in the soil (FAO and GSP, 2020)

Presented below is a guide to the process used for the determination of soil moisture:

1. Select a container that is dry and clean and weigh it.
2. Place the soil sample inside the container and weigh it using the same scale;
3. Oven-dry the sample for 24 hours at 105 ºC;
4. After drying weigh the container with the dried soil.

The following calculation is then done:

$$\text{Water Content } \% = \frac{Ww - Wd}{Ww - Wc} * 100$$

Where:

- Ww = Weight of the wet sample;
- Wd = Weight of the dry sample;
- Wc = Weight of the dried container (without the sample).

The results for soil moisture can be consulted in Appendix II.

3.2.2- Particle size distribution determination

A particle-size analysis is often used to determine soil texture, which can be used to predict hydraulic properties and behaviour in soil, as well as to identify potential contaminants and their distribution in the soil profile (G.W. Gee and J.W. Bauder, 1986).

Particle size distribution (PSD) plays a crucial role in understanding the physical and mechanical behaviour of soils. The distribution of grain sizes provides valuable insights into various aspects of soil, such as its classification, texture, filtration, and overall strength for compaction and stability. Furthermore, particle size distribution determination serves as a valuable indicator of gross particles, particularly those indicative of waste rock (Erguler, 2016).

The purpose of conducting the PSD test is to quantify the distribution of various grain sizes present in a soil sample. This information is used to profile the soil and to predict its behaviour. For this purpose, two methods were used:

1. Sieve analysis;
2. Laser diffraction.

Sieve analysis is a method employed to determine the particle size distribution of soil particles larger than 75 µm in diameter. It involves using a series of stacked sieves with varying sizes

(Figure 6), which, when vibrated, allow finer particles to pass through the openings in each sieve's grid, resulting in the separation of particles based on their size (Hossain et al., 2021). Each set of samples underwent sieving using the Retsch AS200 model with an amplitude of 1.50 mm/''g'' for 15 minutes.

Laser diffraction provides a rapid assessment of the particle size. The instrument measures the changes in light intensity as a laser beam passes through a dispersed soil sample. This method relies on the fact that larger particles scatter light at smaller angles, while smaller particles scatter light at larger angles (Malvern Panalytical, 2023).

Sieve analysis was done through the following:

1. The following sieves were stacked (2 mm, 1mm, 0.425 mm, 150 µm, 106 µm, 75 µm, and base);
2. The instrument was set to an amplitude of 1.50 mm/"g";
3. After 15 minutes the sieves were separated and weight independently;
4. The fraction < 75 µm was separately stored for the laser diffraction analysis;
5. Clean the sieves and repeat for each sample.

Figure 6 – Sieves used for determination of sample textures

Laser diffraction was done along the following steps:

1. Before the analysis, the instrument underwent 2 to 3 cleaning cycles;
2. A small sample of soil ground, below the 75 µm, was carefully placed inside the water tank, ensuring it reached the instrument reading threshold;
3. The instrument measured the sample three times to obtain an average reading;
4. Between each reading, the instrument underwent 1 or 2 additional cleaning cycles to ensure accuracy and prevent any cross-contamination.

3.2.3- Soil pH

The soil pH is measured in terms of hydrogen ion concentration in the solution. This happens when H_2O molecules dissociate into H^+ and OH^- ions. Chemically, pH is defined as the decimal logarithm of the reciprocal of the hydrogen ion activity, H+.

$$\text{pH} = -log_{10}[H^+] = \log\left(\frac{1}{[H^+]}\right) \qquad (1)$$

This is determined using a pH meter, which consists of a pair of electrodes connected to a meter capable of measuring small voltages (in order of the millivolts). The voltage produced by the solution is compared to a known standard buffer solution, and the difference is used to calculate the pH. Minor adjustments may be required due to temperature-induced variations in chemical activity (FAO, 2021). To measure the soil pH, it is necessary to submerge the pH meter in a solution that was in agitation with the soil sample (Figure 7). This immersion allows for direct contact between the instrument's electrode and the soil solution, enabling the pH meter to assess the acidity or alkalinity of the soil.

The procedure for soil pH determination is described here:

1. Weight 10g of soil sample into a beaker and add 20mL of distilled water;
2. Mix the mixture for 60 minutes;
3. Let the suspended particles settle for 30 minutes;
4. Place the electrode into the partially settled suspension to mitigate the suspension effect.

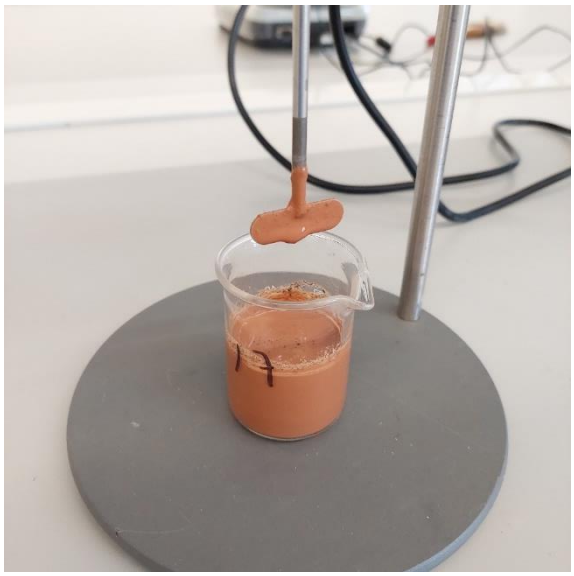

Figure 7 – Sample mixed for pH determination

3.2.4- Static Net Acid Generation

The importance of the Net Acid Generation (NAG) test has been well established. A research project for predicting acid drainage in mine rock and wastes concluded that the NAG test is a simple, inexpensive, and practical method (Miller et al., 1997). The Static Net Acid Generation test is a method used to determine the potential for acid mine drainage in a sample of rock or mine waste. The test involves adding hydrogen peroxide to the sample and then measuring the solution pH after the oxidation is complete. This is done to quantify the amount of acid generated by the sample due to the oxidation of sulfide minerals. The acid released may react with the natural buffering capacity of the sample, and the acidity of the final solution is a direct measure of the net acid generated by the sample (Shu et al., 2001).

The following procedure was performed for the determination of the NAG:

1. Prepare a solution of Sodium Hydroxide (NaOH) with 0.1 and 0.5 M solution. For this test it's also needed a hydrogen peroxide (H_2O_2) solution at 15% w/v;
2. Weigh 2.5 grams of pulverized sample into a 500 ml beaker;
3. Measure 250 ml of a solution of 15% H_2O_2 and add it to the beaker;
4. Place a watch glass on top of the beaker and place the beaker in a fume hood or well-ventilated area;
5. The sample was left oxidating overnight;
6. After the reaction, place the flask on a hot plate and gently heat the sample for a minimum of 2 hours. (Do not allow the sample to dry. Add deionised water as required to maintain the volume constant);

7. After the 2 hours, let the sample cool to room temperature;
8. Rinse any sample that has adhered to the sides of the flask down into the solution with deionised water and complete the 250 ml;
9. Record the pH of the solution (Figure 8). This is referred to as NAGpH;
10. Titrate the solution to pH 4.5 first and 7.0 after, while stirring, with the appropriate NaOH concentration based on NAGpH as follow:
    a. When NAGpH is > 2 à Titrate with 0.10 M NaOH;
    b. When NAGpH is ≤ 2 à Titrate with 0.50 M NaOH.

Following the titration some calculations are needed:

$$NAG = \frac{49 * V * M}{W} \qquad (2)$$

Where:

- NAG = net acid generation (kg H2SO4/tonne);
- V = volume of NaOH used in titration (ml);
- M = concentration of NaOH used in titration (mol/litre);
- W = weight of sample reacted (g).

Figure 8 – NAG pH measurement before titration, using WTW InoLab ph Level 1 ph Meter

3.2.5- Elemental chemical analysis by X-Ray Fluorescence

X-ray Fluorescence Spectrometry is a rapid method for determining the overall elemental composition of soil samples. It involves bombarding the atoms in the sample with high-energy X-rays, which excite the electrons orbiting the atoms. When these excited electrons return to lower energy levels, characteristic X-rays are emitted, allowing the identification and quantification of specific elements in the soil (PDPL, 2013).

Two different sample sizes were analysed using this procedure: higher than 2 mm and lower than 2 mm. Both particle fractions were grounded to 75 µm, to homogenize the soil matrix. The chemical analysis was performed by the XRF Oxford Instruments, model XMDS2726 (Figure 9), using the mining mode.

The protocol for XRF is described below:

1. Oven-dry the sample for approximately 24 hours at 105 °C;
2. Place the sample in a clean bowl and mix the sample thoroughly by stirring and rotating the bowl (homogenisation);

3. Perform three consecutive readings of the sample using the XRF equipment, ensuring to stir the sample between each reading.

Figure 9 – Oxford XRF instrument used for analysis

3.2.6- Total Organic Carbon – *Walkley & Black Method*

The determination of soil total organic carbon is performed using the Walkley & Black chromic acid wet oxidation method. In this method, the organic carbon in the soil is oxidized by a potassium dichromate solution, acidified with concentrated sulfuric acid, raising the temperature of the reaction which is sufficient to induce oxidation. The dichromate reduced during the reaction with soil is proportional to the oxidisable organic carbon present in the sample. Then the solution is back-titrated with ferrous ammonium sulphate, to reduce the remaining dichromate (FAO, 2020). The titration point is visible, since the solution turns into a red-wine colour, due to the usage of a ferroin indicator. In agricultural settings, soil TOC and soil organic matter are essential determinants of soil fertility, quality, and productivity. Although the Wakley-Black method dates back to 1934, it remains a reliable and trusted approach for analysis (Avramidis et al., 2015).

The procedure for the determination of TOC is described here:

1. Weight 1 gram of air-dried soil into a 250 Erlenmeyer flask;
2. Add 10 mL of 0.167 M of $K_2CR_2O_7$ and swirl the flask gently (Figure 10);
3. With care, rapidly add 20 mL concentrated H_2SO_4, directing the stream into the suspension;
4. Immediately swirl the flask gently until the soil and reagents are mixed, then more vigorously for a total of 1 min;
5. Allow the flask to stand on an insulated sheet for 30 minutes in a fume hood;
6. Add 200 mL of deionized water to the flask;
7. Add three to five drops of the Ferroin indicator solution;
8. Titrate with 0.5M of $FeSO_4$ until the solution changes from green to red;
    a. Determine 1-3 blanks in the same manner, without soil.

Figure 10 – Determination of total organic carbon. Samples after addiction of $K_2CR_2O_7$ and before titration

After using the volume of FeSO4, the % of organic carbon that existed in the sample must be calculated according to the following equation:

$$Cr_2O_7 + 3C^0 + 16H^+ \Leftrightarrow 4\ Cr^{3+} + 3\ CO_2 + 8\ H_2O \qquad (3)$$

According to the previous equation, 1 mL of 1 N dichromate solution is equivalent to 3 mg of carbon.

$$Organic\ Carbon\ (\%) = \frac{(Vblank - Vsample) * Mfe * 0.003 * 100 * f * mcf}{W} \quad (4)$$

Where:

- Mfe = concentration of standardized $FeSO_4$ or $(NH_4)_2\ Fe(SO_4)_2.6H_2O$ solution (molarity);
- 0.003 = Stoichiometry Coefficients
  $= \frac{12\text{ g C}}{\text{mole}}$ x $\frac{1\text{ mole } K_2CrO_7}{6\text{ moles } FeSO_4}$ x $\frac{3\text{ moles C}}{2\text{ moles } K_2CrO_7}$ x $\frac{1\text{ L}}{1000\text{ mL}}$
- f = correction factor (1.3);
- w = weight of soil;
- mcf = Moisture correction factor (equal to 1 for dried samples).

4 Results and Discussion

4.1- Granulometry

The particle size distribution analysis was conducted using a combination of sieving and laser diffraction techniques. These methods allowed for a comprehensive characterization of the particle size distribution in all the samples. In agreement with the classification of soil particle size by the United States Department of Agriculture (USDA), the soil was classified as clay (< 0.002 mm), silt (0.002 – 0.05 mm), sand (0.05 – 2 mm) and gravel (2 – 75mm) (USDA-NRCS, 2017). In Figure 11 is presented the particle size distribution of the soil samples, and Appendix III and appendix **Erro! A origem da referência não foi encontrada.** shows the collected data.

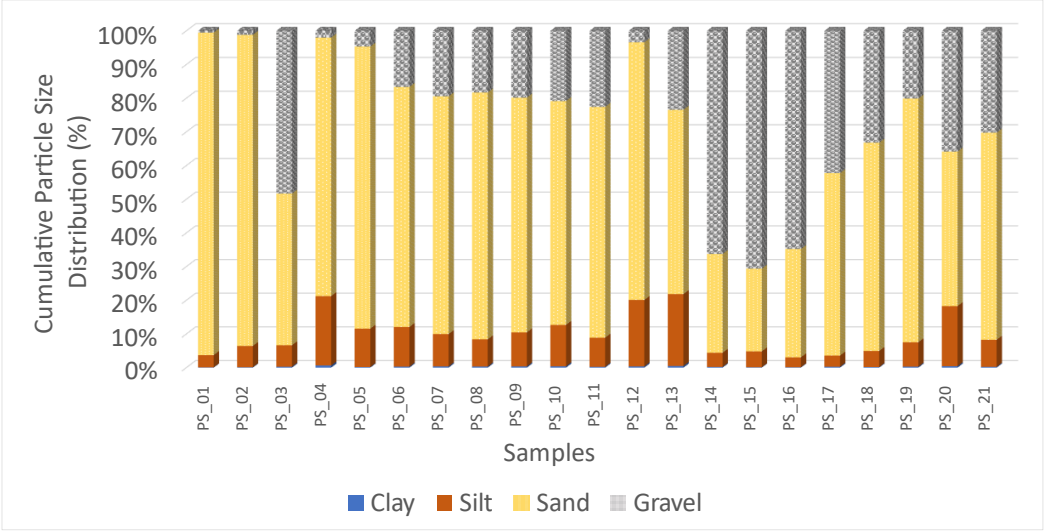

Figure 11 – Cumulative Particle Size Distribution of clay, silt, sand, and gravel classification for the 21 samples

Overall, the samples exhibit a predominant composition of sand, with minimal presence of clay. The silt fraction ranges from 1% to 20%. The presence of gravel in the samples varies significantly, with PS_03, PS_14, PS_15, and PS_16 exhibiting substantial proportions of this coarse fraction.

Tailings deposits are generally fine-grained, primarily due to the type of machinery and equipment used in mining operations (RGC, 2016). According to Panchal, 2018, 77.5% of the tailings, primarily comprise large silt-sized particles ranging from 2 to 75 µm. In contrast, clay-sized particles measuring less than 2 µm account for approximately 4.5% of the tailings, while sand-sized particles up to 4.75 mm make up approximately 18% of the total composition (Panchal et al., 2018).

Samples PS_03, PS_14, and PS_15 exhibit a notable composition with a higher proportion of gravel particles, which could potentially be attributed to the presence of waste rock in those samples. In contrast, the remaining samples demonstrate a significant abundance of sand particles

accompanied by a comparatively lower quantity of silt particles. Despite PS_03 being situated on the opposite side of the river, far away from the mining installations, local reports suggest the presence of waste rock in that area. On the contrary, PS_16 exhibits a notable abundance of coarse soil particles, predominantly gravel. This is because PS_16 originates from a natural rock slope, where the abundance of coarse particles, including gravel, is a natural property.

Samples PS_01 and PS_02 exhibit a significant proportion of sand in their composition. However, this sand accumulation appears to be intentional and controlled by the local municipality, as these samples were collected from a recreational park where people engage in activities such as picnics and other outdoor leisure.

The particle size analysis shows a significant quantity of coarse particles, such as sand, which have a lower surface area and lower water-holding capacity (Wang et al., 2022), which can result in lower adsorption and retention of contaminants. However, it can facilitate the dispersion of contaminants by leaching. In this sense, due to the substantial presence of gravel near the mine, there is a possibility that contaminants from the soil may be leaching into the river. However, the findings from Lopes 2022, indicate that the concentrations of heavy metals in the river do not exhibit an increase from upstream to downstream of the mine.

4.2- Elemental chemical composition (XRF)

To assess the concentration of heavy metals in the collected samples, an XRF analysis was conducted. The test was performed using two size ranges, samples with a particle size of < 2 mm and samples with a particle size of > 2 mm (Appendix V and Appendix I). The concentration of elements between the two size fractions did not exhibit significant differences. Therefore, the analysis focused on the results of the XRF measurements for the fraction with a particle size less than 2 mm, as the majority of the samples fell within this range. In Table 1, it is included a comprehensive selection of elements of interest. The colour scheme assists in distinguishing for each individual element, which samples have lower values, represented in green, and which have higher, depicted in red. Additional elements and values were obtained and can be seen in Appendix V, along with their corresponding error values.

Table 1 - Heavy metals (Zn, Fe, Cu, As, Cd, Sb, and Pb) concentration in mg/kg of dry soil from the XRF analysis for soil particles with a diameter < 2mm. For each element (column), the colour gradient is from green (minimum) to red (maximum).

	Zn [mg/kg]	Fe [mg/kg]	Cu [mg/kg]	As [mg/kg]	Cd [mg/kg]	Sb [mg/kg]	Pb [mg/kg]
PS_01	97	26556					
PS_02	68	26317					
PS_03	95	65663	68		16		105
PS_04	121	36379		52			
PS_05	146	31189		28			
PS_06	99	32052	20	164		340	
PS_07	68	40096		70		92	
PS_08	200	43357		105		131	
PS_09	113	51611		79			
PS_10	324	32772	18	286		1700	214
PS_11	172	47822	31	225		1170	
PS_12	140	41132		62			
PS_13	69	47111	8	128		371	
PS_14	34	81584	9	74		115	
PS_15	37	45082	17	747		2017	177
PS_16	15	42136				116	
PS_17		62715	9	35			
PS_18	65	58535	22				
PS_19	110	41429	45	124		1769	94
PS_20	15	47103		34			
PS_21	94	35336		75	13	120	

The locations of samples PS_15 and PS_10 appear to be the most concerning. PS_15 has a high concentration of heavy metals, including arsenic (747 mg/kg), antimony (2017 mg/kg), and lead (177 mg/kg). PS_10 also presents with arsenic (286 mg/kg), antimony (1700 mg/kg), lead (214 mg/kg), and zinc (324 mg/kg). These concentrations significantly exceed recommended limits for urban soils (Appendix V). Arsenic is considered a toxic element, and its high concentration in both samples raises concerns about potential health risks, especially considering that it is present in a form that is readily available for uptake by plants or direct human exposure

(Mondal et al., 2022). Antimony, in high concentrations, can also have detrimental effects on the environment and organisms, including plants and aquatic life.

Samples PS_01, PS_02, and PS_18 exhibit levels below the respective limits for arsenic, antimony, lead, zinc, copper, and cadmium. These findings suggest that these samples likely possess soil conditions that are considered safe, as their heavy metal concentrations fall within the acceptable range recommended by the APA guidelines. It should be noted that samples PS_03, PS_06, PS_08, PS_12, PS_2,0 and PS_21 show a diverse range of values, with certain elements exceeding the permissible limits defined by regulations.

Samples PS_04, PS_10, and PS_11, originating from agricultural fields, raise significant concerns. Despite these lands being utilized for agriculture, probably with the use of fertilizer and pesticides, and presumably constant disturbance, the presence of heavy metals is alarmingly high. Such contamination not only has the potential to impede plant growth but also poses health risks as these toxic elements can accumulate within plants, posing threats to both human and animal well-being.

PS_16 and PS_17 were collected as possible reference samples from undisturbed soils. There's some distance between the points and in retrospect, additional samples should have been collected in the same locations, nonetheless, they can provide some assumptions about what a standard soil for the region should be. The low concentration of most heavy metals, such as lead, arsenic and antimony indicate that these soils have not been subjected to contamination, nor any impact from mining. This clearly contrasts with the strong presence of the same elements in other collected samples, which suggests that these soils may indeed be undisturbed and can serve as reference points for comparison. Taking this into consideration, when comparing the measured values with the established reference points, it becomes evident that the majority of the samples surpass the specified limits. Notably, PS_16 exhibits no detectable levels of As and its Sb content is among the lowest observed across all collected samples. Similarly, PS_17 demonstrates an absence of Sb and a notably low concentration of As. These findings suggest the possible existence of natural occurrences of these heavy metals in the region. However, they also indicate that a significant portion of the collected samples is contaminated (Figure 12). Human activities, including petrochemical spillages, the use of fertilizers and pesticides, industrial expansion, and wastewater spillages, have contributed to the increasing presence of heavy metals in the soil. Elements such as Fe, Cr, Zn, Cu, Pb, and Cd are among the contaminants responsible for soil contamination (Abhijith L. and Varghese, 2021).

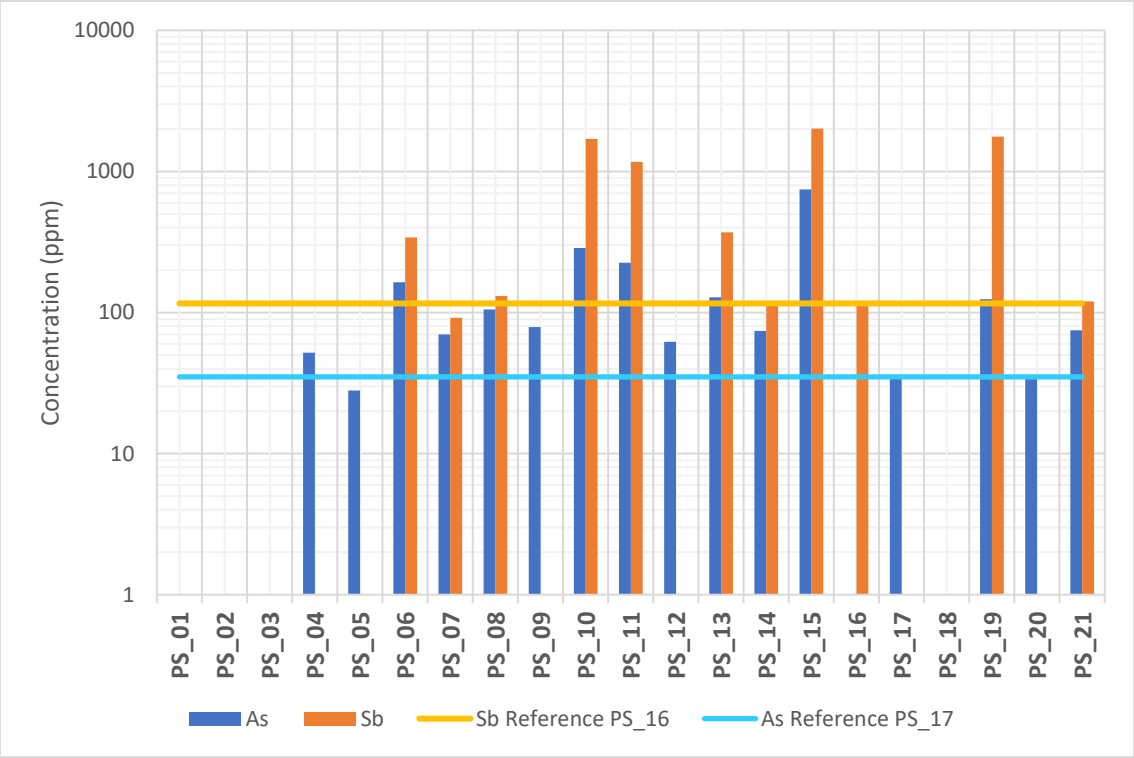

Figure 12 - Concentration of As and Sb compared with reference samples

Copper and zinc are essential nutrients for plants, playing crucial roles in various physiological processes. However, excessive concentrations of these elements can be toxic to both plants and other organisms (Ma et al., 2023). In the presented soil samples, the values for copper generally fall below the limits set by the Portuguese Environmental Agency (APA), table B (Reference values for soil less than 30m from surface water), which can be seen in Appendix V, for both agricultural lands (62 mg/kg) and urban areas (92 mg/kg). This suggests that, except for sample PS_03, the copper levels in the soil are within a suitable range to support healthy plant growth. On the other hand, sample PS_10 exceeds the limit for zinc in soil with a value of 324 mg/kg, as discussed another important element in plant growth.

Certain elements, such as lead, antimony, and arsenic, are well-known for their severe hazards to plants, animals, and humans, even at low concentrations (Jiang et al., 2023). Elevated levels of these elements in the soil can indicate potential contamination and raise concerns about the overall health and safety of the soil. Among the samples, PS_10 stands out with the highest lead concentration, suggesting a potential source of lead contamination in that area. APA value for lead contamination states 45 mg/kg for agricultural soils and 120 mg/kg for urban use. PS_10 has its origin in agricultural soil, so the value of 214 mg/kg surpasses 5 times the threshold established. Similarly, sample PS_15 exhibits the highest antimony value, while also surpassing the limits for antimony in urban areas set by the Portuguese agency. As for arsenic, neither of the

samples is below the 11 mg/kg limit for agricultural soil or 18 mg/kg for urban use, but sample PS_15 exceeds the limit for urban areas by more than 8 times.

It is essential to acknowledge the existence of soils that inherently possess elevated levels of such metals, like arsenic and antimony. Even in the absence of any human activities that could contribute to contamination, these values could surpass the thresholds established by APA. Labelling these soils as contaminated based on their inherent high concentrations would be an oversimplification. However, it is imperative to delve deeper into the matter and underscore the significance of these naturally occurring high concentrations in terms of their potential risks to both the environment and human well-being. Are other site-specific factors such as the geological composition of the land the reason for such established background values or are the origin of this from anthropogenic sources, including agricultural practices, waste disposal, or the use of chemical compounds that can impact the interpretation of results, particularly when multiple sources of contamination exist?

However, in the studied area, where agriculture and livestock production are the predominant activities, it is believed that these factors do not have a great influence on the measured results. Hence, the sites with high concentrations of arsenic and antimony are attributed to mining activities, indicating contamination. In summary, points PS_04 to PS_15, PS_19, and PS_21 are identified as contaminated or moderate contamination.

4.3- Soil pH

The pH measurements were conducted on all 21 samples using deionized water. This water, being neutral with a pH of around 7, facilitates the release of ions and minerals from the soil. Figure 13, below, shows the results obtained when the pH was measured in the 21 collected samples and Appendix III displays the data from the analysis. The black dashed lines mark the boundaries of the range where soil pH is classified as neutral (between 6.6 and 7.3) according to United States Department of Agriculture (USDA) guidelines (USDA, 2022).

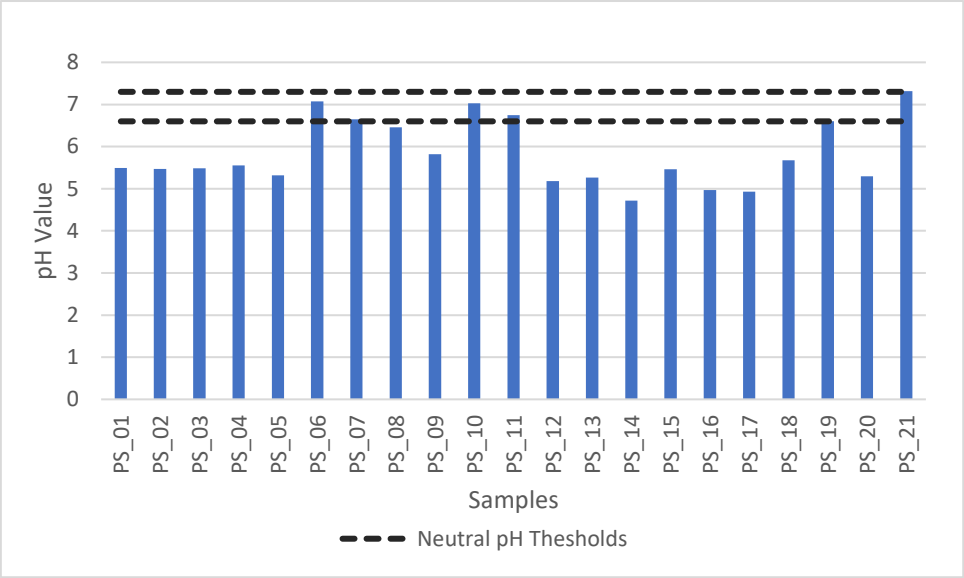

Figure 13 – Soil pH values obtained for the 21 collected samples

The soil pH analysis revealed significant acidity in the soil, as evidenced by 14 samples (PS_01 to PS_ 05, PS_09, PS_11 to PS_18, and PS_20) exhibiting pH levels around 5.5. Of particular concern is sample 14, which recorded a pH of 4.715. On the other hand, the highest pH value observed was 7.318 in sample PS_21, reflecting a near-neutral pH within one of the optimal ranges previously mentioned.

The initial five samples (PS_01 to PS_05), along with PS_18, were collected from the same side of the Sousa River in Covelo. These samples exhibited remarkably similar pH values (mean is 5.5) with a minimal deviation (0.076), independently of their origin and main use. The reference samples (PS_16 and PS_17) that are unaffected by the mine's influence, were obtained from the area above the mine and revealed a pH of around 5.

According to the soil database of Portugal (Infosolos), the pH range of the region's soil is typically between 4.6 and 5.5. When considering non-agricultural areas, the pH values obtained generally align with the expected range presented in the Infosolos database. Notably, some of our sampling points exhibited a more neutral pH value, particularly those in agricultural locations (PS_07 to PS_08, PS_10, PS_11, PS_19, and PS_21), likely due to the application of pH-balancing chemicals, which is a common technique employed by farmers. The findings align with the outcomes of Lopes, 2022.

Soil pH can be an informative measurement for determining soil characteristics in a rapid and informative manner, providing much more information beyond just whether the soil is acidic or basic. By using pH, it is possible to estimate the availability of essential nutrients and the toxicity

of other elements, due to their known relationship with pH (G.W. Thomas, 1996). Still, on its own, soil pH provides limited information, serving mainly as a basis for formulating initial hypotheses that require further confirmation through the analysis of other soil properties. The assessment of heavy metal concentrations may be more significant since it can justify the value of pH determined and proves the presence of harmful substances.

It is worth noting that soil pH naturally fluctuates over time due to factors like seasonal changes (Dong et al., 2022), decreasing climate humidity (Tang et al., 2022), and interactions with external elements. In agriculture, soil pH serves as a fertility indicator, offering insights into nutrient availability and microbial activity. Different pH ranges significantly impact plant growth and the accessibility of essential elements (Johansen et al., 2021). pH values below 5.5 or above 6.5 can negatively affect plant health and nutrient availability, although these thresholds may vary across geographical regions and types of plantations (Thomas, 2018).

Other research findings, suggest that typically plants thrive in soil with a pH ranging from 6.0 to 7.5, as this pH range allows for optimal nutrient availability. Soil with an acidic pH can also increase the mobility of toxic elements, potentially leading to leaching into groundwater or uptake and accumulation in plants (FAO, 2021). Since most samples (PS_01 to PS_05, PS_09, PS_12 to PS_18, and PS_20) are outside of this range, it is determined that this land is not appropriate for agriculture. On the other hand, in soils with higher pH levels, the availability of phosphorus and several micronutrients may decrease, affecting plant growth and development, though none of the samples collected had alkaline values.

The measurement of pH also serves as a valuable indicator of acid mine drainage (AMD) due to its strong correlation with acidity. AMD is formed through the oxidative dissolution of sulfide minerals, characterized by the presence of highly acidic wastewater that contains dissolved metal sulphates and salts. The acidic nature of AMD poses a significant environmental concern as it has the potential to contaminate water sources and disturb ecosystem balances, has heavy metals tend to show higher solubility in soils with acidic pH. Mining activities intensify this process by increasing sulfide mineral exposure. AMD occurs in both active and abandoned mining sites, affecting tunnels, open pits, waste rock piles, and tailings (Simate and Ndlovu, 2014).

4.4- Organic Carbon

Figure 14, shows the values of TOC obtained for the 21 samples collected next to the Montalto mine with Appendix VII showing the results obtained.

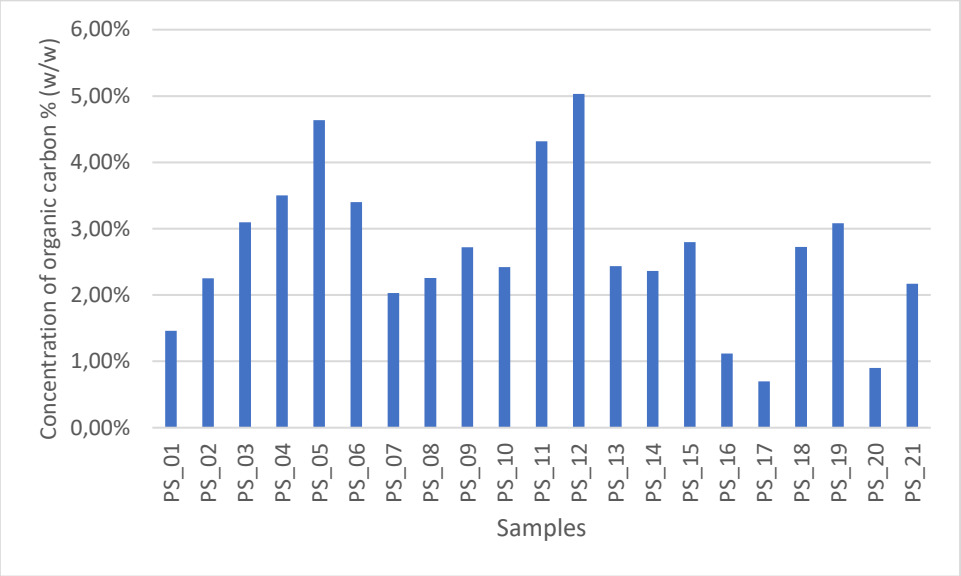

Figure 14 - TOC content in % (w/w) for all 21 samples

Among the analysed samples, PS_12 stands out with the highest percentage of total organic carbon, followed by PS_05 and PS_11. This finding aligns with expectations as PS_12 was collected from a forested area adjacent to a river, where organic matter input and decomposition rates are typically high. On the contrary, the lowest TOC value was observed in sample PS_17, with 0.70%. PS_01 and PS_02 present an unexpected outcome as they originate from a small park area. Despite the significant presence of sand, as indicated by the soil particle distribution analysis, these samples exhibit low levels of TOC (1.46% and 2.25%, respectively).

The article by Haofan X (2021) features a map represented here in Figure 15, which utilizes data from the GEMAS project. The GEMAS project aimed to create a comprehensive soil geochemical dataset for agricultural and grazing land soils across Europe. The soil samples were collected at a depth of 0-20 cm and were composited from five sub-sites within a 10 × 10 m square. On the map, the region of the Porto district exhibits a range of TOC between 3% and 3.5% (Xu and Zhang, 2021). Checking the European Geological Data Infrastructure (EGDI) website, the closest sample to the Montalto area presents a value of 3.3% (EGDI, 2022). The values depicted Figure 15 align with the TOC content measurements obtained from our collected samples.

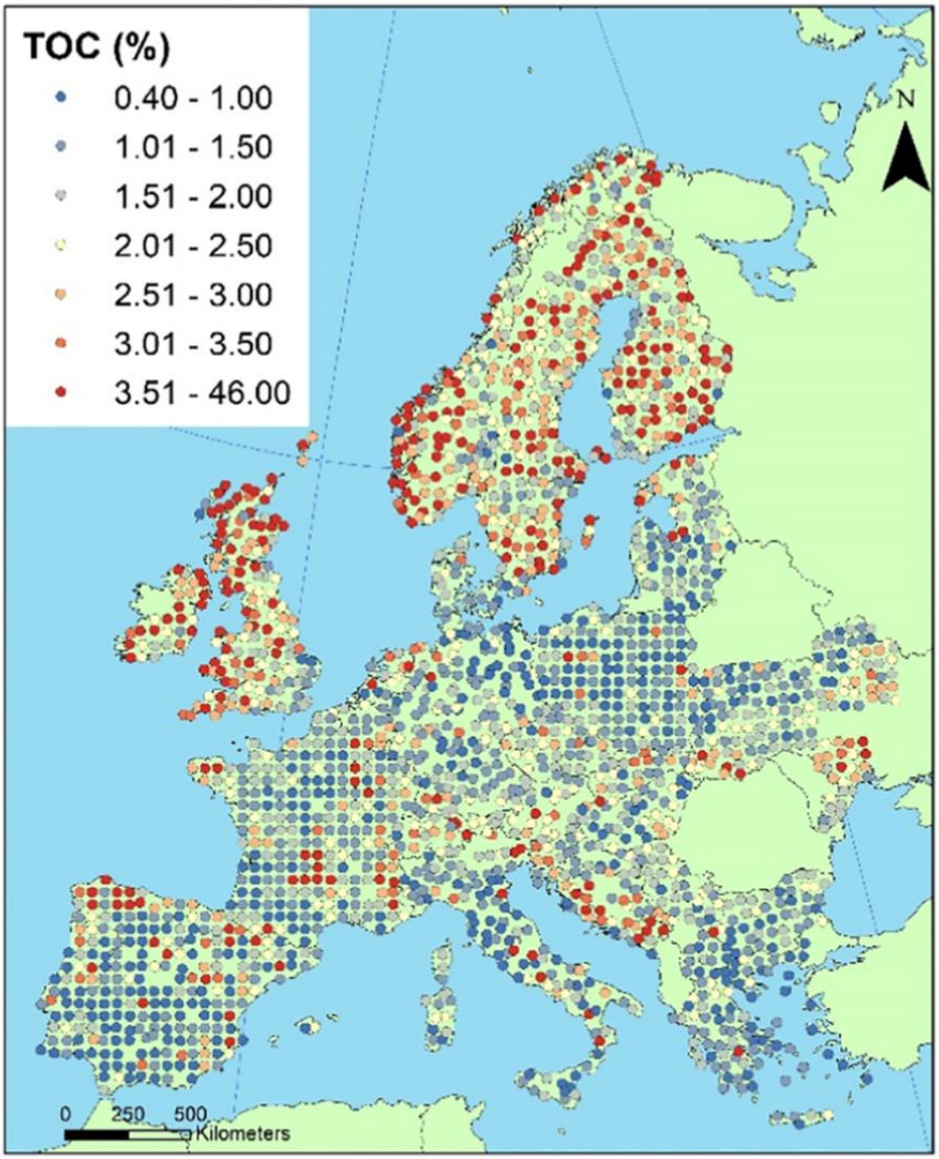

Figure 15 – Map showing agricultural soil sampling locations, with) TOC contents in European agricultural soil samples based on GEMAS project data Extracted from (Xu and Zhang, 2021)

Total organic carbon plays a crucial role in assessing the environmental condition of terrestrial and aquatic ecosystems mainly in soils and sediment fractions. It indicates the organic content derived from various sources such as decomposed plants and animals but also indicates certain anthropogenic factors like chemical contaminants, fertilizers, and organic waste. TOC concentrations are intricately linked to organic contaminants, making it a useful tool for evaluating contamination levels and toxicity (Avramidis et al., 2015). Certain samples (PS_08, PS_09, and PS_10) exhibit a potential connection to fertilizers or other chemicals, as indicated by their significantly low TOC content, despite being associated with farming practices and having a generally neutral pH. Additionally, the presence of tailings in the area might also justify the low TOC content. Sample PS_10 might distinguish itself since it demonstrates high contaminant levels as already discussed, which could be reflected in its low TOC value. However,

it is important to note that these three samples originate from similar land and are located only a few meters apart. Consequently, there is a significant likelihood of contaminants leaching into adjacent areas, raising concerns about potential contamination spread.

The correlation between higher TOC content and fertile soils further supports the importance of preserving and maintaining organic matter in soils. Soil degradation can also lead to a decline in the level of biomass carbon within the soil, primarily due to the erosion of plant litter. This process reduces the soil's resilience by diminishing water content and nutrient availability (Guo et al., 2023). The reference samples (PS_16 and PS_17) exhibit notably low values (1.1% and 0.7% respectively) and are characterized by a significant proportion of gravel-sized particles, which is expected knowing their origin is from a slope where it's difficult for the formation of plant litter and as such the deposition of organic matter.

Amongst all the collected agricultural fields, most of the samples exhibited low values (below 3.5%) of organic matter (OM). It is crucial to implement measures to enhance these values, as there exists a correlation between the content of OM and the concentrations of extractable phosphorus and potassium for plant growth (Alvarenga et al., 2022). This correlation emphasizes the significance of soil organic matter as an indicator of soil quality and fertility. An elevation in TOC content can, for example, be attributed to the addition of organic matter from the plant litter overlay, thereby contributing to the provision of essential ecosystem services. (Guo et al., 2023).

4.5- NAG

Figure 16 shows the values obtained when the NAG test, was applied to all 21 samples for a calibre size of < 2 mm. Samples with a particle size of > 2 mm were also analysed for NAG, which can be seen in Figure 17. The data obtained to establish the results here discussed can be seen in Appendix IX and Appendix X.

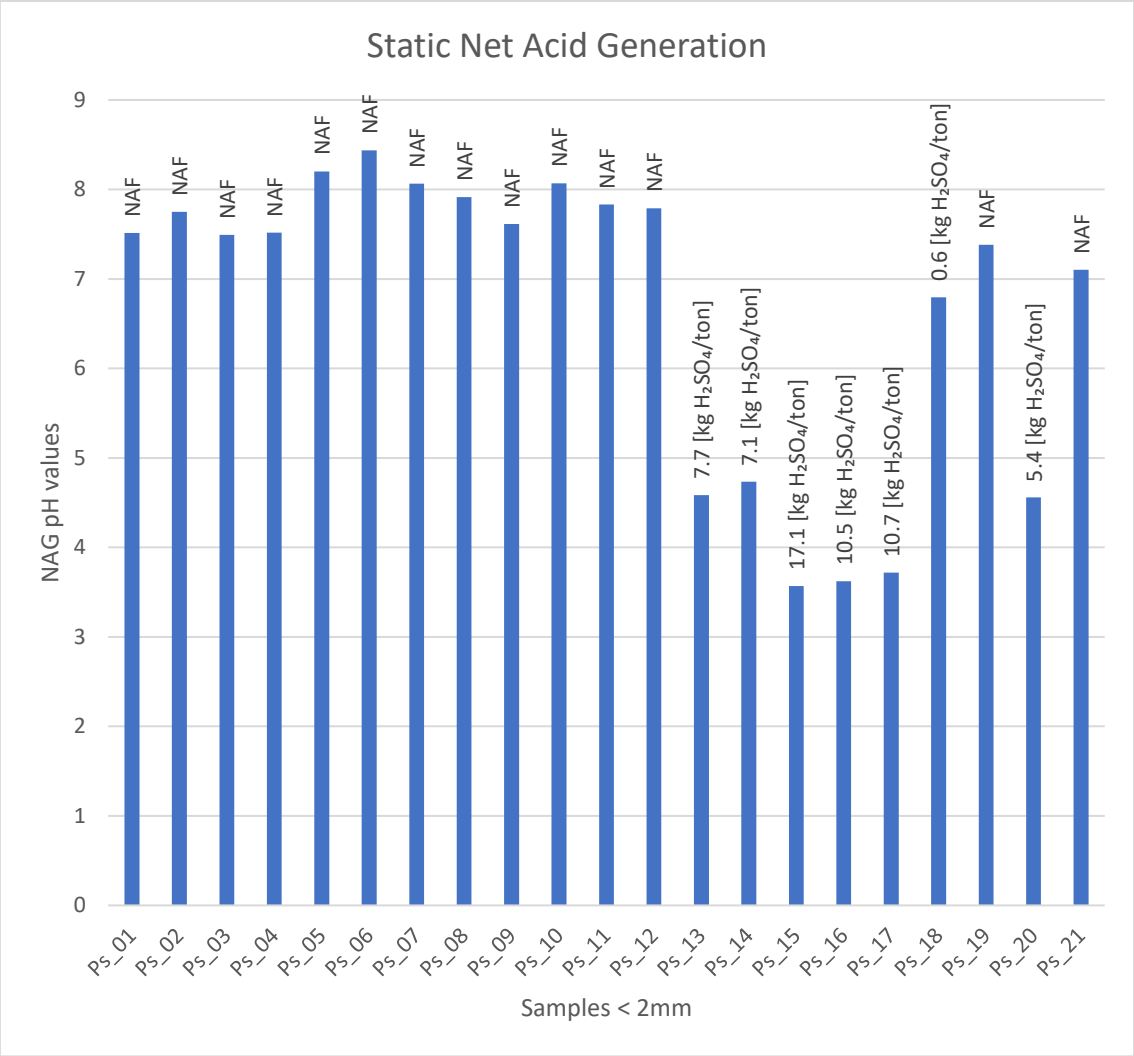

Figure 16 – NAG pH values for samples < 2mm, with acid generated in kg H_2SO_4/ton.

According to the results, samples from Ps_01 to Ps_12, Ps_19, and Ps_21 are reported as Non-Acid Forming (NAF), meaning they do not generate acid or have significant amounts of acid-forming potential. Samples Ps_13, Ps_14, Ps_16, and Ps_17 exhibited significant potential for acid generation, with PS_15 recording the highest value of 17.1 kg H_2SO_4/ton and PS_18 registering the lowest value of 0.6 kg H_2SO_4/ton. A high NAG value indicates that the soil sample has the potential to generate a significant amount of acid when exposed to oxidation conditions. This can have implications for the soil's suitability for agricultural use. However, in the case of the samples collected from agricultural fields, it is fortunate that none of them demonstrated acid-generation characteristics.

It is worth emphasizing that in samples PS_13, PS_14, and PS_15, there is clear evidence of residue deposition originating from mining operations. Consequently, the acidity observed in these locations is concerning as it stems from this deposition. Based on the NAG values indicating acid generation, it can be concluded that the observed acidity is indeed attributed to acid mine

drainage. In samples PS_16 and PS_17, although the potential for acid generation is also high, there is no visual indication of residue deposition. Hence, the acidity observed in these samples can be attributed to natural processes, acid rock drainage, as it represents the inherent phenomenon of acid drainage occurring without any significant human intervention from these two sites.PS_15, PS_16, and PS_17 all resulted in low NAG pH, respectively 3.568, 3.622, and 3.719 which reveals the connection between NAG pH and the amount of NAG in the samples. PS_18 and PS_03 originate from the same vicinity, just a few meters apart, so the considerably lower NAG value observed in sample PS_18 is consistent with the non-acid-forming nature of sample PS_03, as their NAG pH values were closely aligned. Based on the close proximity of these samples, it can be inferred that their potential for acid generation is similar, with sample 18 showing a decreased likelihood of acid generation.

For the fraction > 2mm, the presence of NAG was noticeable although the values were generally lower (Figure 17). NAG testing was not conducted for samples PS_01, PS_02, PS_04, and PS_05 due to the absence of particles in this fraction.

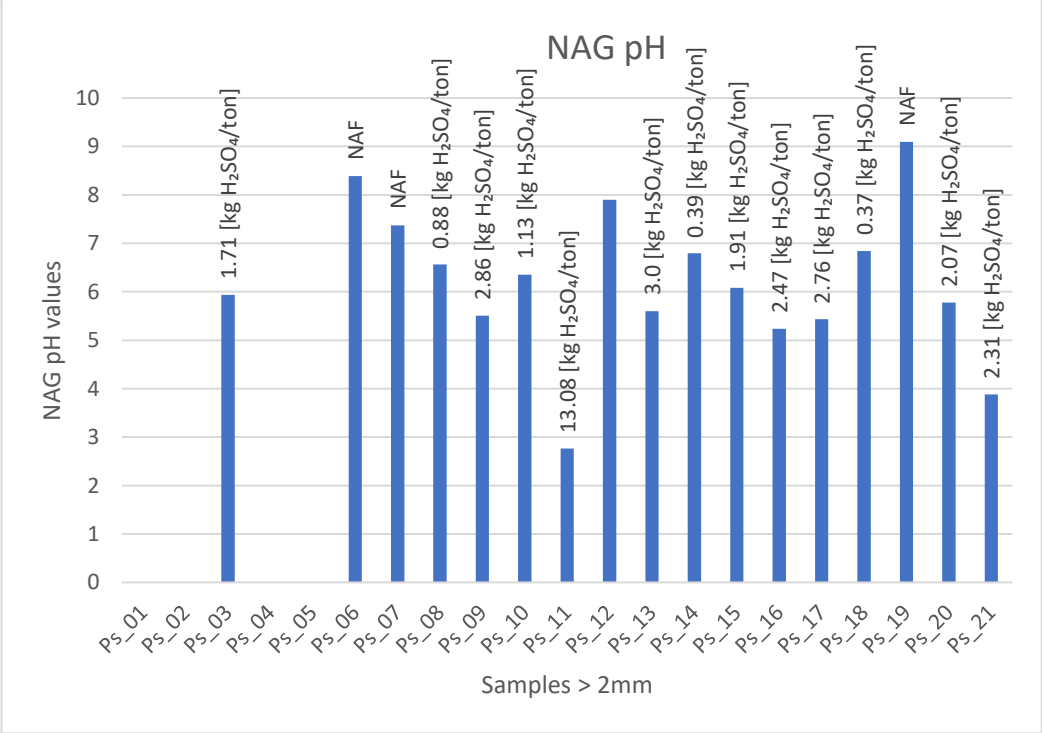

Figure 17 - NAG pH values for samples > 2mm, with acid generated in kg H2SO4/ton

For NAG > 2 mm, the discrepancy in the results could potentially be attributed to the grinding process that the samples underwent. The grinding may have exposed smaller particles, within the larger stones, that had not yet undergone oxidation. Consequently, these smaller particles could react with H_2O_2 during the NAG test, resulting in the release of slight acidity. Notably, PS_11

exhibited a remarkable acid generation potential, generating 13.08 kg H_2SO_4/ton. This high NAG value is unexpected and raises some questions though, at the moment, is difficult to justify such value. Consequently, when a sample exhibits acid generation, it leads to soil acidification, potential acidification of water resources, and the release of heavy metals. This is due to the direct correlation between acidity and the solubility of heavy metals, meaning that higher levels of acidity result in increased heavy metal solubility (Król et al., 2020).

4.6- Global Analysis

The particle size distribution analysis revealed that the samples varied in their composition. Some samples, such as PS_01, PS_02, PS_04, PS_05, and PS_12 showed a distinct presence of sand, while others like PS_14, PS_15, and PS_16 were predominantly composed of gravel particles. Overall, all the results showed a very coarse composition with most samples being composed of both fractions.

XRF analysis indicated varying concentrations of heavy metals across the samples. In PS_15 and PS_10, elevated levels of arsenic, antimony, and lead were observed, indicating contamination. The absence of lead, along with moderate concentrations of arsenic and antimony, were found in PS_04, PS_05, and PS_20. In contrast, PS_01, PS_02 and PS_18 showed concentrations within established regulatory limits.

The majority of the collected samples exhibited pH values below 6.6, indicating a slightly acidic environment. Notably, PS_14 stood out with an exceptionally low pH of 4.715, representing the most acid sample. On the other hand, PS_21 displayed the highest pH value of 7.318, although it still falls within the neutral range. Several other samples also distinguish themselves in this characteristic. Both PS_17 and PS_16, reference samples, showed pH values below 5.0. Also surprisingly, despite being among the most, heavy metal, contaminated samples, PS_10 exhibited a neutral pH of 7.027.

Regarding organic carbon content, the samples demonstrated different levels. Samples like PS_05 and PS_11 exhibited relatively high organic carbon content (4.6% and 4.3%, respectively) with PS_12 reaching 5%, while others like PS_20 had lower levels reaching 0.7%. Considering PS_16 and PS_17 origin, it was expected low levels of organic carbon (1.02% e 0.7%, respectively) since a coarse composition and a slope are not the best sites for easy organic growth. It would be anticipated that PS_13 (2.44%) and PS_14 (2.36%) would exhibit similar values to the reference samples, however, the proximity of a forested area and the slope's instability

contribute to the presence of organic matter infiltrating the soil on the slope. As a result, these samples deviate from the expected values and demonstrate slightly higher organic matter content.

Significant acid generation potential was observed in samples such as PS_15 (17.1 kg H_2SO_4/t), PS_16 (10.5 kg H_2SO_4/t), and PS_17 (10.7 kg H_2SO_4/t), as indicated by their high values. Samples PS_13 (7.7 kg H_2SO_4/t), PS_14 (7.1 kg H_2SO_4/t), PS_18 (0.6 kg H_2SO_4/t), and PS_20 (5.4 kg H_2SO_4/t) also showed some acid generation potential but at lower levels. However, many of the collected samples did not exhibit significant signs of acid formation, which is a positive outcome. This suggests that the majority of the samples are unlikely to generate AMD through leaching. Nevertheless, it is concerning that sample PS_15 stood out once again with elevated values, considering the already alarming levels of contaminants present in this particular sample.

In summary, the results demonstrate significant variations among the samples analysed. Figure 18 shows the outcome in a visual format.

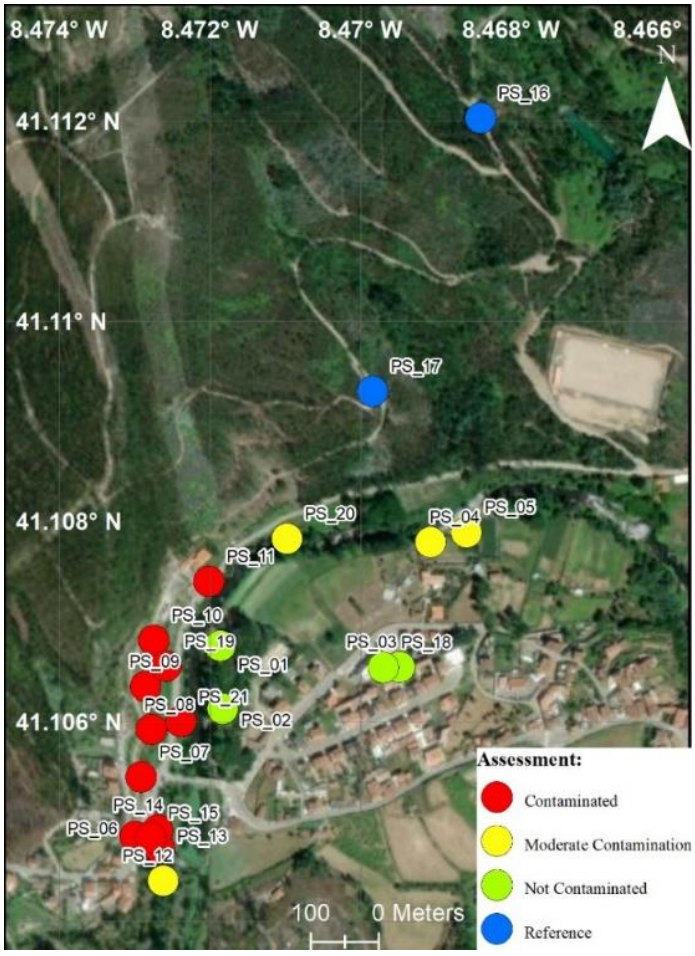

Figure 18 - Map colour code with results.

The green samples are categorized as uncontaminated and do not require any form of treatment. The yellow samples indicate a low level of contamination within acceptable limits. Although they exhibit some degree of contamination, it is not significantly higher than the established thresholds, and they may naturally return to normal levels without the need for remediation. The red samples represent highly contaminated areas and are of great concern among the samples analysed, requiring ongoing remediation and assessment. The blue samples correspond to the reference samples used for comparison and will not be classified.

PS_16 and PS_17 serve as reference samples in our study. These samples are positioned at a substantial distance from the mining area and situated in a less frequented region, with no anthropogenic activity. Their pH values are 4.967 and 4.93, respectively, within an acceptable range for the region. In terms of TOC, PS_16 exhibits a value of 1.12%, while PS_17 demonstrates a lower value of 0.70%. This is expected considering their origin from a heap with a predominance of coarse particles, mainly gravel, and sand, with relatively low levels of silt and clay making it difficult for OM to set and grow. Regarding acid generation potential, both PS_16 and PS_17 show some level, with values of 10.5 kg H_2SO_4/t and 10.7 kg H_2SO_4/t, respectively. However, this occurrence can be attributed to natural processes, specifically acid rock drainage. In terms of contamination, these reference samples do not present significant levels of heavy metals. PS_16 shows no detectable presence of As but displays a low concentration of Sb at 116 mg/kg. Conversely, PS_17 demonstrates no measurable levels of As but exhibits a relatively low concentration of Sb at 35 mg/kg. This contrast holds significant importance as it aids in recognizing the natural presence of these elements and facilitates comparison with other soil samples that show higher levels of contamination by the same heavy metals.

Samples P_01 and P_02, from the leisure park, situated near to each other, where presumed to be not contaminated, for being located on the opposite side of the river. Despite their relatively low organic carbon content (1.46% and 2.25% respectively), due to the human deposition of sands at the site, these samples demonstrate a low concentration of heavy metals. Moreover, both samples display a pH level consistent with the local soil pH range of 4.6-5.5 and exhibit no evidence of acid generation. So, they are classified as not contaminated.

Samples PS_03 and PS_18, both obtained from the children's park, yielded unexpected results that merit attention. Initial concerns arose regarding PS_03 due to indications of waste rock, which could suggest potential contamination. Furthermore, the first analysis revealed the presence of lead at a level of 105 mg/kg, raising further concerns. However, it is important to note that this value remains below the legal limit of 120 mg/kg for urban areas, as stipulated by APA guidelines. In contrast, PS_18 exhibited normal levels of concentrations, with no detectable contamination.

Both samples displayed pH levels within the normal range of the region (5.473 and 5.557, respectively) and demonstrated good TOC values. Additionally, there were no signs of acid generation or elevated levels of heavy metals. This could be attributed to the maintenance and care the area receives, resulting in the presence of green topsoil. Therefore, these samples can also be classified as uncontaminated.

The region encompassing the former mine facilities is represented in samples PS_06 to PS_11, which are now used for housing and agriculture. They raise significant concerns due to the findings indicating a highly contaminated zone with elevated levels of antimony, arsenic, and lead. The soil first presents a better picture, with moderate to high TOC content (from 2% to 4%), the absence of acid drainage, and pH levels within the neutral range (all the pH are above 6.4, except for sample PS_09 with 5.82). However, this assessment can be attributed to agricultural practices aimed at achieving soil pH balance and the utilization of these soils for farming. Despite these favourable aspects, the presence of heavy metals in the area has a major impact and prevails over any other factors since the contamination levels observed are exceptionally high, exceeding both legislative guidelines and reference sample values. Among the samples, PS_10 is highlighted as being the only sample with the presence of Pb (214 mg/kg) surpassing the APA established limits. In conclusion, all the samples pertaining to the mine facilities are categorized as contaminated.

Samples PS_13, PS_14, and PS_15, with origin a few meters apart, exhibit clear signs of contamination, including low pH values, acid generation, and the presence of high concentrations of heavy metals. When the area was first observed, the presence of tailings in the heap was evident, further supporting the assumption of contamination. Notably, these samples demonstrate the lowest pH values among all collected samples, with PS_14 reaching a pH of 4.715. The occurrence of acid generation in all samples indicates their potential to contribute to acid drainage with PS_15 reaching 17.09 kg H_2SO_4/t, posing a significant environmental concern. Furthermore, all three samples exhibit elevated levels of arsenic and antimony, surpassing both legal limits and reference sample values. Of particular concern is sample PS_15, which records the highest concentration of antimony and arsenic among all collected samples, with 2017 mg/kg and 747 mg/kg, respectively. These findings unequivocally establish these samples as contaminated.

Samples PS_04, PS_05, PS_12, and PS_20 are classified as having moderate contamination levels. These samples demonstrate relatively normal pH values within the expected range, as well as high TOC content. Among them, sample PS_12 stands out with the highest TOC value at 5.03%, which aligns with its location within a vegetation-rich area. However, PS_12 raises concerns due to the presence of elevated levels of arsenic, surpassing the concentrations found in

the reference samples. This finding may be attributed to its proximity to the area where samples PS_13, PS_14, and PS_15 were collected, which could potentially result in runoff and the dispersal of contaminated soil particles towards the PS_12 location. On a positive note, PS_12 does not exhibit any signs of acid generation, indicating a lack of acid drainage potential. For PS_20, this sample presents arsenic levels exceeding the APA limits but falling below the reference samples. It also demonstrates some degree of mine acid generation, potentially explaining its pH value of 5.294 and relatively low TOC content of 0.90%. Nevertheless, compared to the other samples, PS_20 remains one of the least contaminated in terms of heavy metals. Samples PS_04 and PS_05 were collected from close proximity but offer distinct backgrounds. PS_04 originates from an agricultural field, while PS_05 is obtained from a river margin. Both samples display pH values within the normal range for the region (5.5 and 5.3, respectively), high TOC content (3.50% and 4.64%), and no evidence of acid drainage. As for arsenic levels, both samples have the element present in their composition with PS_04 having a slightly higher value at 52 mg/kg, surpassing the limit for agricultural soils according to APA guidelines.

Samples PS_19 and PS_21 represent agricultural fields situated in the vicinity of the mine. PS_19 is located at the base of the mine facilities, while PS_21 is situated on the other side of a local road. Neither sample exhibits any indications of acid generation, implying a lack of potential for acid drainage. Both samples exhibit the presence of heavy metals, with PS_19 standing out for its notably high Sb concentration, ranking among the highest values observed among all collected samples (1769 mg/kg). As anticipated, these agricultural fields demonstrate a strongly neutral pH, with PS_19 measuring 6.6 and PS_21 measuring 7.3. Additionally, these display high levels of TOC, with PS_19 reaching 3.08% and PS_21 measuring 2.17%. In conclusion, both samples are contaminated.

4.7- Mitigation measures

Mitigating and remediating the environmental impacts caused by mining activities is of utmost importance and requires careful attention. As mentioned earlier, when around a mining area that has been or is currently active, it is necessary to develop a comprehensive plan that incorporates the best practices throughout all operational phases to address the impacts effectively. Given the broad range of areas affected by mining activities, there are several measures available to tackle all the different challenges in each environmental compartment. In the context of this work, it is essential to explore strategies aimed specifically at enhancing soil quality. The significance of the soil in the Montalto mine area and its surroundings cannot be overstated, particularly for the welfare of the local population. This region holds immense value

due to the generations of families dedicated to agriculture and livestock practices that heavily rely on the quality and health of the soil. It serves as the foundation of their livelihoods, sustains the local economy, and represents a rich cultural heritage from the mine workers.

First, is necessary to emphasize the importance of gaining a deeper understanding of the risks associated with metals found in mine wastes to implement effective soil treatment approaches. By comprehending these risks, suitable remediation strategies can be employed to address soil contamination. One such approach is the removal of the topsoil layer for future use in organic amendments and biofertilizers, which can enhance the revegetation process by promoting the growth of native plant species. This helps in restoring vegetation cover and ecosystem functionality. Additionally, there are biological and chemical stabilization methods for overburden dumps, which aim to improve the stability and long-term sustainability of waste disposal areas (Singh and Singh, 2016).

One other solution is phytoremediation. It is considered an important approach for mitigating soil contamination resulting from mining activities that liberate metal and metalloid pollutants that are known to be cytotoxic, mutagenic, and carcinogenic. Phytoremediation is described as a cleaner, low-cost, and ecologically friendly technology since it uses plants, such as trees and grasses that not only help in soil decontamination but also facilitate the recovery of certain metals. The growth of vegetation can also prevent future soil erosion and the leaching of metals. For such reasons, phytoremediation has gained a positive perception from society, being its only disadvantage the slow growth rates exhibited by most naturally occurring metal hyperaccumulators (Cárdenas-Aguiar et al., 2020; Prasad, 2003).The addition of biochar to phytoremediation and other methods in mitigating environmental risks in gold mining tailings improved various soil properties and reduced the bioavailability of As in the tailings. In a study (Dias et al., 2022), different types of biochar were tested, with palm kernel cake biochar showing the highest efficiency. The chemical properties of biochar, particularly the levels of phosphorus and mineral components played a significant role in reducing As solubility and making it less bioavailable by up to 17% and up to 20% in cyanidation mining tailings

Electrokinetic remediation is a well-established technology used for the remediation of heavy metal-contaminated soil, particularly with fine-grain. It involves the application of electric fields and the utilization of various components to efficiently remove heavy metals. These components include a power supply for electric fields, electrodes, electrolytes, and ion exchange membranes. The effectiveness of electrokinetic remediation relies on the proper functioning and interaction of these components. This method is safe, efficient, simple, and cost-effective but there is a requirement for a conducting pore fluid in the soil mass (Acar et al., 1995; Wang et al., 2021).

Another option is soil washing. This is an effective technique used to remediate contaminated soil. Its main goal is to reduce the volume of polluted soil by concentrating the contaminants in a smaller fraction, thereby making the rest of the soil cleaner. This process involves various methods such as separating the soil particles based on their size and weight and scrubbing them. Sometimes, chemical additives are also used to enhance the cleaning process. In the case of heavy metals, the focus is often on isolating the finer particles due to the higher specific surface area, organic matter, and oxyhydroxide gels, which tend to bind heavy metals. By targeting these particles, the mobility of the metals can be controlled through precipitation, diffusion, volatilization, and dissolution into less harmful forms. Soil washing is known for its efficiency and relatively fast results. However, it should be noted that this technique can be costly due to the equipment and resources required for the process (Sierra et al., 2010).

Regarding the soil of the Montalto's mine vicinity, it becomes evident that soil washing is not a viable option due to its high cost. As a result, alternative approaches such as phytoremediation, coupled with the application of biochar, should be taken into consideration. This method has the potential to effectively decontaminate the soil, recover valuable metals, and restore vegetation cover, thereby mitigating future soil erosion and metal leaching. However, it is crucial to acknowledge that phytoremediation is a gradual process, and for agricultural purposes, long-term remediation technologies may not be practical. Among the available options, electrokinetic remediation emerges as the most promising solution for addressing soil contamination with heavy metals in the Montalto mine area, extensive research has demonstrated its effectiveness in similar contexts. However, its application in the Montalto mine area should be carefully assessed based on site-specific factors and cost-effectiveness. Further research is needed to gain a deeper understanding of the soil properties before implementing electrokinetic remediation as it may not be feasible in the presence of metallic deposits.

4.8- Future Works

For future studies, it is important to explore various aspects related to the characterization of the soil in the Montalto mine area and its surroundings. Further investigations can focus on assessing the potential risks to human health and the potential loss of biodiversity in both soil and aquatic ecosystems. Studies can be conducted to analyse the exposure risks for individuals residing in the area, particularly concerning the concentration of contaminants in animals and agricultural products, which can have implications for human consumption.

Additionally, ecotoxicology studies can be conducted to evaluate the impact of contaminants on the local flora and fauna. Understanding how these contaminants affect the surrounding ecosystem is crucial for the preservation of biodiversity and the overall ecological balance.

Attention should also be given to the outlines of the zones designated for the disposal of tailings. Conducting in-depth drilling and investigations can provide valuable insights into the potential environmental impact and long-term stability of these disposal sites.

Another important aspect to consider is the assessment of the social dimension, particularly the population's awareness of the risks posed by previous mining activities. Understanding the community's perception and knowledge of these risks is essential for effective communication and mitigation strategies. This knowledge can inform targeted educational programs and interventions to enhance awareness and empower the population in dealing with the aftermath of mining.

5- Conclusion

In conclusion, this study aimed to assess the contamination levels and potential environmental risks associated with the studied area. The objectives were to analyse particle size distribution, heavy metal concentrations, soil pH, organic carbon content, and acid generation potential across the collected samples to determine the soil quality in the Montalto mine vicinity. These have been accomplished by providing a comprehensive assessment of the soil quality in the studied area.

The findings of this study have provided valuable information regarding the composition and contamination levels of the studied area. The analysis of particle size distribution revealed a predominantly coarse composition, which promotes contaminant mobility and the potential for soil erosion. Additionally, the XRF analysis unveiled the presence of contamination in specific samples, with varying concentrations of heavy metals. When considering these results alongside NAG, there is a concern regarding the possibility of acid mine drainage. This issue is particularly significant for samples collected within the mining facilities that are currently utilized for agricultural and residential purposes. Overall, 4 samples are considered not contaminated (PS_01, PS_02, PS_03 and PS_18), 4 are described as moderately contaminated (PS_04, PS_05, PS_13 and PS_21), and the other eleven samples are contaminated. Samples PS_16 and PS_17, are considered reference samples and as such were not attributed a classification. The identification of contaminated sites, particularly in the former mine facilities area, highlights the urgent need for remediation measures to mitigate potential risks to human health and the environment.

Analysing all samples proves to be challenging due to their diverse origins and functions within the same region. The location of samples is diverse, with some originating from within the mine facilities, while others are found in parks or urban areas. The different land uses and human activities, like agriculture or leisure, further complicate the analysis. The presence of cultivation crops, maintenance of parks and urban areas, or other human interference all contribute to the complexity of drawing concise conclusions for the entire region. Given these variations, it becomes evident that the region cannot be considered homogeneous due to the diverse land use practices and functions, and varying soil conditions exhibited by each sampled area. Each sample represents a distinct environment with a unique set of factors influencing contamination levels and soil properties. Therefore, any generalization or overarching conclusion about the entire region could be misleading. The presence of multiple contamination sources in the area demands a more comprehensive and nuanced approach in future studies, as mining alone does not account for all the observed contamination. However, the assessment of heavy metals through XRF analysis emerged as the fundamental factor in this study. By comparing the measured values with

the thresholds established by APA and, crucially, with the reference samples, it was possible to discern the sites that exhibited contamination from heavy metals. Based on the specific characteristics and locations of the sites, the results strongly indicate that the concentration of heavy metals is attributed to the mining activity.

Based on the findings, several recommendations can be made. First, remediation efforts should be prioritized in the highly contaminated zones, focusing on reducing heavy metal concentrations and minimizing the risk of leaching. The highest contaminated areas can be situated closest to the mine vicinity and on the same side of the Sousa River. Ongoing monitoring of the area is crucial to track the effectiveness of remedial actions and ensure the long-term sustainability of the environment. Additionally, public awareness campaigns should be conducted to inform the local population about the potential risks associated with contaminated food consumption. Promoting safe and healthy agricultural practices, such as soil testing, proper irrigation, and selection of suitable crops, can help reduce the uptake of contaminants into the food chain.

6- References

Abhijith L., Varghese, E.M., 2021. Removal of zinc and copper from contaminated soil by using adsorbents and mulches. p. 030005. https://doi.org/10.1063/5.0066408

Acar, Y.B., Gale, R.J., Alshawabkeh, A.N., Marks, R.E., Puppala, S., Bricka, M., Parker, R., 1995. Electrokinetic remediation: Basics and technology status. J Hazard Mater 40. https://doi.org/10.1016/0304-3894(94)00066-P

Addo, A.M., Nyantakyi, E.K., Appiah-Adjei, E., Ackerson, N.O.B., Yeboah, S.I.I.K., Borkloe, J.K., Domfeh, M.K., Siabi, E.K., Wezenamo, C.A., Owusu, M., 2023. Environmental and health impacts of mining: a case study in Kenyasi-Ahafo Region, Ghana. Arabian Journal of Geosciences 16, 334. https://doi.org/10.1007/s12517-023-11424-y

Alvarenga, P., Mourinha, C., Palma, P., Cruz, N., Rodrigues, S.M., 2022. Assessment of Soil Physicochemical Characteristics and As, Cu, Pb and Zn Contamination in Non-Active Mines at the Portuguese Sector of the Iberian Pyrite Belt. Environments 9, 105. https://doi.org/10.3390/environments9080105

Araujo, F., Taborda Llano, I., Nunes, E., Santos, R., 2022. Recycling and Reuse of Mine Tailings: A Review of Advancements and Their Implications. https://doi.org/10.20944/preprints202207.0010.v3

Avramidis, P., Nikolaou, K., Bekiari, V., 2015. Total Organic Carbon and Total Nitrogen in Sediments and Soils: A Comparison of the Wet Oxidation – Titration Method with the Combustion-infrared Method. Agriculture and Agricultural Science Procedia 4, 425–430. https://doi.org/10.1016/j.aaspro.2015.03.048

Candeias, C., Ávila, P.F., Ferreira da Silva, E., Ferreira, A., Salgueiro, A.R., Teixeira, J.P., 2014. Acid mine drainage from the Panasqueira mine and its influence on Zêzere river (Central Portugal). Journal of African Earth Sciences 99, 705–712. https://doi.org/10.1016/j.jafrearsci.2013.10.006

Cárdenas-Aguiar, E., Ruiz, B., Fuente, E., Gascó, G., Méndez, A., 2020. Improving Mining Soil Phytoremediation with Sinapis alba by Addition of Hydrochars and Biochar from Manure Wastes. Waste Biomass Valorization 11, 5197–5210. https://doi.org/10.1007/s12649-020-00999-2

Carvalho, A., 1970. Minas de Antimónio e Ouro de Gondomar. Estudos, Notas e Trabalhos do S. F. M XIX.

Carvalho, P., Neiva, A., Silva, M., 2013. Antimony and arsenic behaviours in soils from three abandoned gold mining areas in northern Portugal.

Carvalho, P., Neiva, A., Silva, M., 2012. Assessment to the potential mobility and toxicity of metals and metalloids in soils contaminated by old Sb-Au and As-Au mines (NW Portugal). Environ Earth Sci 65, 1215–1230. https://doi.org/10.1007/S12665-011-1370-8

Carvalho, P., Neiva, A., Silva, M., Silva, E., 2014. Geochemical comparison of waters and stream sediments close to abandoned Sb-Au and As-Au mining areas, northern Portugal. Geochemistry 74, 267–283. https://doi.org/10.1016/J.CHEMER.2013.08.003

Clifford, M.J., Perrons, R.K., Ali, S.H., Grice, T.A., 2018. Extracting Innovations: Mining, Energy, and Technological Change in the Digital Age, First. ed. CRC Press, United States.

Couto, H., 2013. THE ORDOVICIAN IN VALONGO ANTICLINE (NORTHERN PORTUGAL): STATE OF ART. https://doi.org/10.5593/SGEM2013/BA1.V1/S01.028

Couto, H., 1993. As mineralizações de Sb-Au da região Dúrico-Beirã. FCUP, Porto.

Desogus, P., Manca, P.P., Orrù, G., Zucca, A., 2013. Stabilization–solidification treatment of mine tailings using Portland cement, potassium dihydrogen phosphate and ferric chloride hexahydrate. Miner Eng 45, 47–54. https://doi.org/10.1016/j.mineng.2013.01.003

Dias, Y.N., Pereira, W.V. da S., Costa, M.V. da, Souza, E.S. de, Ramos, S.J., Amarante, C.B. do, Campos, W.E.O., Fernandes, A.R., 2022. Biochar mitigates bioavailability and environmental risks of arsenic in gold mining tailings from the eastern Amazon. J Environ Manage 311, 114840. https://doi.org/10.1016/j.jenvman.2022.114840

Dixon-Hardy, D.W., Engels, J.M., 2007. Methods for the disposal and storage of mine tailings. Land Contamination & Reclamation 15, 301–317. https://doi.org/10.2462/09670513.832

References

Dong, Y., Yang, J.-L., Zhao, X.-R., Yang, S.-H., Mulder, J., Dörsch, P., Zhang, G.-L., 2022. Seasonal dynamics of soil pH and N transformation as affected by N fertilization in subtropical China: An in situ 15N labeling study. Science of The Total Environment 816, 151596. https://doi.org/10.1016/j.scitotenv.2021.151596

EDM, DGEG, 2011. The legacy of abandoned mines : the context and action in Portugal, 1st ed.

EGDI, 2022. European Geological Data Infrastructure [WWW Document]. URL https://www.europe-geology.eu (accessed 5.20.23).

Erguler, Z.A., 2016. A quantitative method of describing grain size distribution of soils and some examples for its applications. Bulletin of Engineering Geology and the Environment 75, 807–819. https://doi.org/10.1007/s10064-015-0790-1

Eurostat, 2023. Statistics Explained - Waste statistics [WWW Document]. URL https://ec.europa.eu/eurostat/statistics-explained/index.php?title=Waste_statistics#Total_waste_generation (accessed 5.29.23).

FAO, 2021. Standard operating procedure for soil pH determination. Rome.

FAO, 2020. Standard operating procedure for soil organic carbon. Walkley-Black method: titration and colorimetric method. Rome.

FAO, GSP, 2020. Soil testing methods manual. FAO, Rome. https://doi.org/10.4060/ca2796en

Fernández-Lozano, J., Palao-Vicente, J.J., Blanco-Sánchez, J.A., Gutiérrez-Alonso, G., Remondo, J., Bonachea, J., Morellón, M., González-Díez, A., 2019. Gold-bearing Plio-Quaternary deposits: Insights from airborne LiDAR technology into the landscape evolution during the early Roman mining works in north-west Spain. J Archaeol Sci Rep 24, 843–855. https://doi.org/10.1016/j.jasrep.2019.03.001

Ferreira da Silva, E., Almeida, S.F.P., Nunes, M.L., Luís, A.T., Borg, F., Hedlund, M., de Sá, C.M., Patinha, C., Teixeira, P., 2009. Heavy metal pollution downstream the abandoned Coval da Mó mine (Portugal) and associated effects on epilithic diatom communities. Science of The Total Environment 407, 5620–5636. https://doi.org/10.1016/j.scitotenv.2009.06.047

Fiúza, A., Futuro, A., Gois, J., Dinis, M.L., Vila, C., Carvalho, S., Fernandes, A., 2023. The Legacy of Potential Environmental Soil Contamination in an Antimony Mining Heritage Area. Minerals 13, 257. https://doi.org/10.3390/min13020257

Goclawska, J.A., USGS, 2022. The Mineral Industry of Portugal in 2017-2018.

Grangeia, C., Ávila, P., Matias, M., da Silva, E.F., 2011. Mine tailings integrated investigations: The case of Rio tailings (Panasqueira Mine, Central Portugal). Eng Geol 123, 359–372. https://doi.org/10.1016/j.enggeo.2011.10.001

Guo, L., Xiong, S., Chen, Y., Cui, J., Yang, S., Wang, H., Wang, Y., Ding, Z., 2023. Total organic carbon content as an early warning indicator of soil degradation. Sci Bull (Beijing) 68, 150–153. https://doi.org/10.1016/j.scib.2023.01.012

G.W. Gee, J.W. Bauder, 1986. Particle-size analysis, Second. ed.

G.W. Thomas, 1996. Soil pH and soil acidity, 1st ed. SSSA–ASA.

Hilson, G., Nayee, V., 2002. Environmental management system implementation in the mining industry: a key to achieving cleaner production. Int J Miner Process 64, 19–41. https://doi.org/10.1016/S0301-7516(01)00071-0

Hossain, S., Islam, A., Badhon, F.F., Imtiaz, T., 2021. Properties and Behavior of Soil – Online Lab Manual. Mavs Open Press.

Hu, Y., Yu, Z., Fang, X., Zhang, W., Liu, J., Zhao, F., 2020. Influence of Mining and Vegetation Restoration on Soil Properties in the Eastern Margin of the Qinghai-Tibet Plateau. Int J Environ Res Public Health 17, 4288. https://doi.org/10.3390/ijerph17124288

Inverno, C., Augusto, F., Matos, J., 2020. MAPPING OF MINERAL DEPOSITS OF PORTUGAL, 1:200 000 SCALE [WWW Document]. LABORATÓRIO NACIONAL DE ENERGIA E GEOLOGIA, IP. URL https://www.lneg.pt/wp-content/uploads/2021/10/CDM-MAP-URMG2021_LNEG-Policy-brief-2021_EN.pdf (accessed 6.3.23).

Jenkins, H., Yakovleva, N., 2006. Corporate social responsibility in the mining industry: Exploring trends in social and environmental disclosure. J Clean Prod 14, 271–284. https://doi.org/10.1016/j.jclepro.2004.10.004

References

Jiang, M., Wang, K., Li, G., Zhao, Q., Wang, W., Jiang, J., Wang, Y., Yuan, L., 2023. Stabilization of arsenic, antimony, and lead in contaminated soil with montmorillonite modified by ferrihydrite: Efficiency and mechanism. Chemical Engineering Journal 457, 141182. https://doi.org/10.1016/j.cej.2022.141182

Johansen, J.L., Nielsen, M.L., Vestergård, M., Mortensen, L.H., Cruz-Paredes, C., Rønn, R., Kjøller, R., Hovmand, M., Christensen, S., Ekelund, F., 2021. The complexity of wood ash fertilization disentangled: Effects on soil pH, nutrient status, plant growth and cadmium accumulation. Environ Exp Bot 185, 104424. https://doi.org/10.1016/j.envexpbot.2021.104424

Julio, C., 2008. Com o Projecto Lombador, Neves-Corvo será a segunda maior mina de zinco da Europa. O Campaniço (75) 10–11.

Król, A., Mizerna, K., Bożym, M., 2020. An assessment of pH-dependent release and mobility of heavy metals from metallurgical slag. J Hazard Mater 384, 121502. https://doi.org/10.1016/j.jhazmat.2019.121502

Kundu, M., Das, T., Biswas, P., Mondal, S., Ghosh, G., 2017. Effect of different land uses on soil organic carbon in new alluvial belt of West Bengal. International Journal of Bio-Resource, Environment and Agricultural Sciences 3, 517–520.

Kusi-Sarpong, S., Bai, C., Sarkis, J., Wang, X., 2015. Green supply chain practices evaluation in the mining industry using a joint rough sets and fuzzy TOPSIS methodology. Resources Policy 46, 86–100. https://doi.org/10.1016/j.resourpol.2014.10.011

Lazorenko, G., Kasprzhitskii, A., Shaikh, F., Krishna, R.S., Mishra, J., 2021. Utilization potential of mine tailings in geopolymers: Physicochemical and environmental aspects. Process Safety and Environmental Protection 147, 559–577. https://doi.org/10.1016/j.psep.2020.12.028

Leite, M.R.M., Silva, A.F. da, 2013. Mineral raw materials, concepts, upgrading and potential in Portugal. Ciência & Tecnologia dos Materiais 25, 71–74. https://doi.org/10.1016/j.ctmat.2014.03.001

Lima, A., Matías Rodríguez, R., Fonte, J., 2015. A Exploração de Depósitos Secundários de ouro nas Serras de Santa Justa e Pias (Município de Valongo).

Lopes, F., 2022. Assessment of Contamination Potential and Environmental Risk Characterization - The Case Study of The Resources Affected by Former Sb Mine of Montalto. FEUP, Porto.

Loveland, P., 2003. Is there a critical level of organic matter in the agricultural soils of temperate regions: a review. Soil Tillage Res 70, 1–18. https://doi.org/10.1016/S0167-1987(02)00139-3

Ma, XinYue, Ma, XiaoLi, Chen, P., 2023. The Effect of Microplastics-Plants on the Bioavailability of Copper and Zinc in the Soil of a Sewage Irrigation Area. Bull Environ Contam Toxicol 110, 58. https://doi.org/10.1007/s00128-022-03674-5

Malvern Panalytical, 2023. Laser Diffraction (LD) [WWW Document]. URL https://www.malvernpanalytical.com/en/products/technology/light-scattering/laser-diffraction#:~:text=Laser%20diffraction%20measures%20particle%20size,scatter%20light%20at%20large%20angles (accessed 6.3.23).

Mencho, B.B., 2022. Assessing the effects of gold mining on environment: A case study of Shekiso district, Guji zone, Ethiopia. Heliyon 8, e11882. https://doi.org/10.1016/j.heliyon.2022.e11882

Miller, S., Robertson, A., Donahue, T., 1997. Advances in acid drainage prediction using the net acid generating (NAG) test, in: Fourth International Conference on Acid Rock Drainage. Vancouver.

Mondal, S., Pramanik, K., Ghosh, S.K., Pal, P., Ghosh, P.K., Ghosh, A., Maiti, T.K., 2022. Molecular insight into arsenic uptake, transport, phytotoxicity, and defense responses in plants: a critical review. Planta 255, 87. https://doi.org/10.1007/s00425-022-03869-4

Moreno, L., Neretnieks, I., 2006. Long-term environmental impact of tailings deposits. Hydrometallurgy 83, 176–183. https://doi.org/10.1016/j.hydromet.2006.03.052

Munanku, T., Banda, K., Nyimbili, P.H., Mhlongo, S.E., Masinja, J., 2023. Development of a multi-criteria decision analysis tool for the assessment of the potential pollution risk of

tailings dumps to the environment – An approach validated using selected Zambian Mine tailings. Journal of African Earth Sciences 200, 104880. https://doi.org/10.1016/j.jafrearsci.2023.104880

Neiva, A.M.R., Andráš, P., Ramos, J.M.F., 2008. Antimony quartz and antimony–gold quartz veins from northern Portugal. Ore Geol Rev 34, 533–546. https://doi.org/10.1016/J.OREGEOREV.2008.03.004

Pacheco-Torgal, F., 2015. Introduction to eco-efficient masonry bricks and blocks, in: Eco-Efficient Masonry Bricks and Blocks. Elsevier, pp. 1–10. https://doi.org/10.1016/B978-1-78242-305-8.00001-2

Panchal, S., Deb, D., Sreenivas, T., 2018. Mill tailings based composites as paste backfill in mines of U-bearing dolomitic limestone ore. Journal of Rock Mechanics and Geotechnical Engineering 10, 310–322. https://doi.org/10.1016/j.jrmge.2017.08.004

PDPL, 2013. Analysis of Soil Samples Using a Portable X-Ray Fluorescence Spectrometry (XRF).

Prasad, M.N.V., 2003. Phytoremediation of Metal-Polluted Ecosystems: Hype for Commercialization. Russian Journal of Plant Physiology. https://doi.org/10.1023/A:1025604627496

Prasadini, P., Mohan, M., 2019. Manual on Practical Soil Physics. Associate Director of Research Regional Agricultural Research Station Tirupati – 517 502, India.

Real, J.P., 2016. A evolução técnica nas Minas da Panasqueira em 120 anos de actividade.

RGC, 2016. Physical and Geochemical Characteristics of Waste Rock and Contaminated Materials .

Schoenberger, E., 2016. Environmentally sustainable mining: The case of tailings storage facilities. Resources Policy 49, 119–128. https://doi.org/10.1016/j.resourpol.2016.04.009

Segui, P., Safhi, A. el M., Amrani, M., Benzaazoua, M., 2023. Mining Wastes as Road Construction Material: A Review. Minerals 13, 90. https://doi.org/10.3390/min13010090

Seki, H.A., Thorn, J.P.R., Platts, P.J., Shirima, D.D., Marchant, R.A., Abeid, Y., Baker, N., Annandale, M., Marshall, A.R., 2022. Indirect impacts of commercial gold mining on adjacent ecosystems. Biol Conserv 275, 109782. https://doi.org/10.1016/j.biocon.2022.109782

Shu, W.S., Ye, Z.H., Lan, C.Y., Zhang, Z.Q., Wong, M.H., 2001. Acidification of lead/zinc mine tailings and its effect on heavy metal mobility. Environ Int 26, 389–394. https://doi.org/10.1016/S0160-4120(01)00017-4

Sierra, C., Gallego, J.R., Afif, E., Menéndez-Aguado, J.M., González-Coto, F., 2010. Analysis of soil washing effectiveness to remediate a brownfield polluted with pyrite ashes. J Hazard Mater 180, 602–608. https://doi.org/10.1016/j.jhazmat.2010.04.075

Silva, G., 2017. A Indústria Mineira no Distrito do Porto no final do século XIX: o antimónio nos concelhos de Valongo e Gondomar. FLUP, Porto.

Simate, G.S., Ndlovu, S., 2014. Acid mine drainage: Challenges and opportunities. J Environ Chem Eng 2, 1785–1803. https://doi.org/10.1016/j.jece.2014.07.021

Sims, I., Lay, J., Ferrari, J., 2019. Concrete Aggregates, in: Lea's Chemistry of Cement and Concrete. Elsevier, pp. 699–778. https://doi.org/10.1016/B978-0-08-100773-0.00015-0

Singh, P.K., Singh, R.S., 2016. Environmental and Social Impacts of Mining and their Mitigation. National Seminar.

Svobodova, K., Owen, J.R., Kemp, D., Moudrý, V., Lèbre, É., Stringer, M., Sovacool, B.K., 2022. Decarbonization, population disruption and resource inventories in the global energy transition. Nat Commun 13, 7674. https://doi.org/10.1038/s41467-022-35391-2

Tang, K., Li, F.Y., Jaesong, S., Liu, Y., Sun, T., Liu, J., Gao, X., Wang, Y., 2022. Soil water retention capacity surpasses climate humidity in determining soil organic carbon content but not plant production in the steppe zone of Northern China. Ecol Indic 141, 109129. https://doi.org/10.1016/j.ecolind.2022.109129

Thomas, G.W., 2018. Soil pH and Soil Acidity. pp. 475–490. https://doi.org/10.2136/sssabookser5.3.c16

References

USDA, 2022. Soil Health - pH [WWW Document]. URL https://www.nrcs.usda.gov/sites/default/files/2022-11/pH%20-%20Soil%20Health%20Guide_0.pdf (accessed 6.2.23).

USDA-NRCS, 2017. Soil Survey Manual, USDA Handbook 18. Gov. Printing Office 18.

Wang, X.-Q., Zhang, X.-C., Pei, X.-J., Ren, G.-F., 2022. Effect of the Particle Size Composition and Dry Density on the Water Retention Characteristics of Remolded Loess. Minerals 12, 698. https://doi.org/10.3390/min12060698

Wang, Y., Li, A., Cui, C., 2021. Remediation of heavy metal-contaminated soils by electrokinetic technology: Mechanisms and applicability. Chemosphere 265, 129071. https://doi.org/10.1016/j.chemosphere.2020.129071

Worlanyo, A.S., Jiangfeng, L., 2021. Evaluating the environmental and economic impact of mining for post-mined land restoration and land-use: A review. J Environ Manage 279, 111623. https://doi.org/10.1016/j.jenvman.2020.111623

Xu, H., Zhang, C., 2021. Investigating spatially varying relationships between total organic carbon contents and pH values in European agricultural soil using geographically weighted regression. Science of The Total Environment 752, 141977. https://doi.org/10.1016/j.scitotenv.2020.141977

Yilmaz, E., Koohestani, B., Cao, S., 2023. Recent practices in mine tailings' recycling and reuse, in: Managing Mining and Minerals Processing Wastes. Elsevier, pp. 271–304. https://doi.org/10.1016/B978-0-323-91283-9.00013-4

Zhang, W., Alakangas, L., Wei, Z., Long, J., 2016. Geochemical evaluation of heavy metal migration in Pb–Zn tailings covered by different topsoils. J Geochem Explor 165, 134–142. https://doi.org/10.1016/j.gexplo.2016.03.010

7- Appendixes

I. Sampling sites

Table 2 - Sampling sites data with GPS location and early expectations

Sampling site	Date	Expectation	GPS_3_ marker	Lat	Long
PS_01	14/02/2023	Without contamination	116	41,10676	-8,47187
			117	41,10675	-8,47186
			118	41,10675	-8,47186
PS_02	14/02/2023	Without contamination	113	41,10612	-8,47184
			114	41,10613	-8,47183
			115	41,10613	-8,47182
PS_03	14/02/2023	Contaminated	122	41,10652	-8,46948
			123	41,10654	-8,46949
			124	41,10657	-8,46949
PS_04	14/02/2023	Without contamination	125	41,10779	-8,46907
			126	41,10779	-8,46907
			127	41,1078	-8,46909
PS_05	14/02/2023	Without contamination	128	41,10787	-8,46869
			129	41,1079	-8,46855
			130	41,1079	-8,46855
PS_06	14/02/2023	Unknown	137	41,10483	-8,47298
			138	41,10486	-8,47299
			139	41,10486	-8,473
PS_07	14/02/2023	Unknown	140	41,10545	-8,47291
			141	41,10544	-8,47292
			142	41,10544	-8,47291
PS_08	14/02/2023	Unknown	143	41,10592	-8,47277
			144	41,10592	-8,47278
			145	41,10591	-8,47278
PS_09	14/02/2023	Unknown	146	41,10635	-8,47285
			147	41,10635	-8,47285
			148	41,10634	-8,47287
PS_10	14/02/2023	Unknown	149	41,1068	-8,47275
			150	41,10681	-8,47275
			151	41,10682	-8,47274
PS_11	14/02/2023	Unknown	152	41,1074	-8,47201
			153	41,1074	-8,47201
			154	41,1074	-8,47202

Appendixes

Sampling site	Date	Expectation	GPS_3_ marker	Lat	Long
PS_12	14/02/2023	Without contamination	155	41,10442	-8,47262
			156	41,1044	-8,47262
			157	41,1044	-8,47262
PS_13	14/02/2023	Contaminated	158	41,10474	-8,47267
			159	41,10474	-8,47268
			160	41,10474	-8,47267
PS_14	14/02/2023	Contaminated	161	41,1049	-8,47269
			162	41,10492	-8,4727
			163	41,10492	-8,47269
PS_15	14/02/2023	Contaminated	164	41,10483	-8,4728
			165	41,10484	-8,47279
			166	41,10484	-8,47279
PS_16	16/02/2023	Reference	170	41,11204	-8,46841
			171	41,11203	-8,46841
			172	41,11203	-8,46841
PS_17	17/02/2023	Reference		41,63361	-8,281187
				41,63361	-8,281187
				41,63361	-8,281187
PS_18	18/02/2023	Contaminated	173	41,10654	-8,4697
			174	41,10654	-8,4697
			175	41,10654	-8,4697
PS_19	19/02/2023	Unknown	179	41,10685	-8,4723
			180	41,10682	-8,4723
			181	41,10681	-8,47231
PS_20	20/02/2023	Unknown	182	41,10783	-8,47098
			183	41,10783	-8,47098
			184	41,10782	-8,47098
PS_21	21/02/2023	Unknown	185	41,10598	-8,4724
			186	41,106	-8,47239
			187	41,10601	-8,47237

II. Soil Moisture

Table 3 – Experimental data of the soil moisture determination.

Sample	Recipient (g)	Recipient + Wet sample (g)	Recipient + Dry sample (g)	Moisture (g)	Original Sample (g)	Water Content (%)
PS_01	767	1724	1609	115	957	12%
PS_02	771	1831	1644	187	1060	18%
PS_03	305	1896	1642	254	1591	16%
PS_04	995	1957	1730	227	962	24%
PS_05	750	1875	1575	300	1125	27%
PS_06	761	1658	1503	155	897	17%
PS_07	305	1401	1227	174	1096	16%
PS_08	357	1334	1176	158	977	16%
PS_09	768	1828	1663	165	1060	16%
PS_10	771	1760	1580	180	989	18%
PS_11	775	1772	1575	197	997	20%
PS_12	761	1761	1455	306	1000	31%
PS_13	357	1343	1176	167	986	17%
PS_14	757	1814	1733	81	1057	8%
PS_15	768	2487	2382	105	1719	6%
PS_16	765	1747	1610	137	982	14%
PS_17	303	1278	1070	208	975	21%
PS_18	304	1507	1290	217	1203	18%
PS_19	762	1569	1391	178	807	22%
PS_20	766	1739	1563	176	973	18%
PS_21	745	1648	1511	137	903	15%

III. Particle Size (Sieve)

Table 4 - Particle size determination through sieving

min size (mm)	PS_01	PS_02	PS_03	PS_04	PS_05	PS_06	PS_07	PS_08	PS_09	PS_10	PS_11
4,75	100%	100%	100%	100%	100%	100%	100%	100%	100%	100%	100%
2	100%	100%	64%	100%	100%	100%	100%	100%	100%	100%	100%
1	99%	99%	52%	98%	95%	83%	81%	82%	80%	79%	77%
0,425	97%	94%	40%	95%	84%	71%	69%	66%	67%	65%	67%
0,15	47%	58%	27%	84%	73%	44%	44%	40%	44%	43%	44%
0,106	9%	17%	13%	43%	39%	22%	18%	18%	21%	24%	18%
0,075	5,504%	10,407%	8,332%	29,420%	24,408%	16,433%	12,321%	10,890%	14,200%	17,852%	12,014%
< 0,075	3%	7%	6%	21%	15%	12%	8%	6%	10%	13%	8%

min size (mm)	PS_12	PS_13	PS_14	PS_15	PS_16	PS_17	PS_18	PS_19	PS_20	PS_21
4,75	100%	100%	100%	100%	100%	100%	100%	100%	100%	100%
2	100%	100%	100%	47%	100%	100%	100%	100%	100%	100%
1	97%	77%	34%	29%	35%	58%	67%	80%	64%	70%
0,425	91%	65%	23%	22%	21%	34%	46%	62%	51%	53%
0,15	78%	49%	15%	16%	12%	20%	28%	38%	40%	31%
0,106	49%	33%	9%	10%	6%	8%	12%	17%	28%	16%
0,075	30,674%	27,032%	5,047%	6,663%	3,894%	3,918%	6,271%	9,291%	23,330%	10,442%
< 0,075	20%	23%	4%	5%	2%	1%	3%	5%	19%	7%

Appendixes

IV. Particle Size (Sieving Results)

Table 5 –– Proportion of soil particles according to the diameter Ranges (mm) of the USDA classification.

Sample	PS_01	PS_02	PS_03	PS_04	PS_05	PS_06	PS_07	PS_08	PS_09	PS_10	PS_11
Clay	0%	0%	0%	1%	0%	0%	0%	0%	0%	0%	0%
Silt	4%	6%	6%	21%	11%	12%	10%	8%	10%	12%	9%
Sand	96%	92%	45%	77%	84%	71%	71%	73%	70%	66%	69%
Gravel	1%	1%	48%	2%	5%	17%	19%	18%	20%	21%	23%
Sample	PS_12	PS_13	PS_14	PS_15	PS_16	PS_17	PS_18	PS_19	PS_20	PS_21	
Clay	0%	1%	0%	0%	0%	0%	0%	0%	0%	0%	
Silt	20%	21%	4%	5%	3%	3%	5%	7%	18%	8%	
Sand	76%	55%	29%	25%	32%	54%	62%	72%	46%	61%	
Gravel	3%	23%	66%	71%	65%	42%	33%	20%	36%	30%	

V. XRF Results For The Soil Fraction With a Particle Size Below 2 mm

Table 6 - XRF results of samples fraction with a particle size < 2mm, with values in % and +/- representing the standard deviation

Sample	K (%)	+/-	Ca (%)	+/-	Ti (%)	+/-	Mn (%)	+/-	Fe (%)	+/-	Ni (%)	+/-	Cu (%)	+/-	Zn (%)	+/-
PS_01					0,3294	0,0502	0,014	0,0099	2,6556	0,2676					0,0097	0,0018
PS_02					0,3292	0,0325	0,0129	0,0091	2,6317	0,2977					0,0068	0,0004
PS_03					0,6328	0,0486	0,0438	0,0107	6,5663	0,2528			0,0068	0,0026	0,0095	0,0015
PS_04					0,4418	0,0183	0,0378	0,0037	3,6379	0,1778					0,0121	0,0019
PS_05					0,4284	0,0547	0,0382	0,0047	3,1189	0,289					0,0146	0,0024
PS_06					0,3505	0,0572	0,0253	0,0065	3,2052	0,5436	0,0017	0,0012	0,002	0,0016	0,0099	0,0022
PS_07					0,4256	0,0216	0,0336	0,0041	4,0096	0,1358					0,0068	0,0009
PS_08					0,473	0,0217	0,0521	0,0111	4,3357	0,0579					0,02	0,0007
PS_09					0,568	0,0131	0,0217	0,0078	5,1611	0,2131					0,0113	0,0008
PS_10					0,3488	0,0139	0,0254	0,0024	3,2772	0,0462	0,0008	0,0011	0,0018	0,0014	0,0324	0,0009
PS_11	0,7732	1,0935	0,1447	0,2046	0,4751	0,0273	0,0719	0,0044	4,7822	0,2441			0,0031	0,0026	0,0172	0,0023
PS_12					0,4902	0,0143	0,0564	0,0071	4,1132	0,0259					0,014	0,0012
PS_13					0,4011	0,0106	0,0214	0,0038	4,7111	0,0317			0,0008	0,0012	0,0069	0,0005
PS_14					0,3468	0,0175	0,1088	0,0014	8,1584	0,1987			0,0009	0,0012	0,0034	0,0003
PS_15					0,3517	0,0725	0,0489	0,0047	4,5082	0,7201			0,0017	0,0013	0,0037	0,001
PS_16					0,6738	0,0584			4,2136	0,4107					0,0015	0,001
PS_17	0,084	0,1188			0,4339	0,0453			6,2715	0,5915			0,0009	0,0013		
PS_18					0,5965	0,0959	0,0258	0,011	5,8535	0,7892			0,0022	0,0016	0,0065	0,0008
PS_19					0,4308	0,1069	0,0309	0,0063	4,1429	0,8911			0,0045	0,0016	0,011	0,0035
PS_20					0,4487	0,0831			4,7103	0,8007					0,0015	0,0014
PS_21					0,3364	0,0555	0,0326	0,0052	3,5336	0,5357					0,0094	0,0017

Appendixes

Sample	As (%)	+/-	Rb (%)	+/-	Sr (%)	+/-	Y (%)	+/-	Zr (%)	+/-	Nb (%)	+/-	Mo (%)	+/-	Cd (%)	+/-
PS_01			0,0286	0,0034	0,0144	0,0018	0,0018	0,0003	0,024	0,003	0,0024	0,0002	0,0017	0,0001		
PS_02			0,0252	0,0031	0,013	0,0017	0,002	0,0002	0,0278	0,0042	0,0023	0,0001	0,0015	0,0003		
PS_03			0,0134	0,0008	0,0043	0,0003	0,0044	0,0002	0,0358	0,0031	0,0022	0,0003	0,0018	0,0004	0,0016	0,0023
PS_04	0,0052	0,0004	0,0265	0,0022	0,0128	0,001	0,0029	0,0005	0,0393	0,003	0,0027	0,0001	0,0013	0,0002		
PS_05	0,0028	0,002	0,027	0,0033	0,015	0,0015	0,0032	0,0002	0,0552	0,0049	0,0028	0,0003	0,0015	0,0003		
PS_06	0,0164	0,0039	0,0177	0,0038	0,0108	0,0025	0,0024	0,0007	0,0244	0,0061	0,0019	0,0004	0,0012	0,0008		
PS_07	0,007	0,0004	0,0183	0,0008	0,0096	0,0002	0,0029	0,0002	0,0298	0,0021	0,0025	0,0002	0,0017	0,0002		
PS_08	0,0105	0,0002	0,0197	0,0001	0,0084	0,0001	0,0039	0,0001	0,0334	0,0009	0,0027	0,0003	0,0017	0,0001		
PS_09	0,0079	0,0001	0,0153	0,0013	0,0069	0,0002	0,0034	0,0001	0,0345	0,0036	0,0025	0,0004	0,0024	0,0007		
PS_10	0,0286	0,0012	0,0177	0,0005	0,0112	0,0005	0,0025	0,0002	0,0294	0,0009	0,0024	0,0003	0,0016	0		
PS_11	0,0225	0,0008	0,0209	0,001	0,0126	0,0005	0,0035	0,0001	0,0367	0,0021	0,0024	0,0001	0,0017	0,0001		
PS_12	0,0062	0,0006	0,0283	0,0005	0,0138	0,0002	0,0041	0,0003	0,0533	0,002	0,0029	0,0002	0,0014	0,0002		
PS_13	0,0128	0,0003	0,0132	0,0003	0,0058	0,0002	0,003	0,0003	0,0225	0,0004	0,0022	0,0002	0,0017	0,0001		
PS_14	0,0074	0,0006	0,0113	0,0001	0,0078	0,0001	0,0036	0,0002	0,0258	0,0011	0,0019	0,0001	0,0022	0,0002		
PS_15	0,0747	0,0137	0,0076	0,0014	0,0064	0,0011	0,0029	0,0004	0,0211	0,003	0,0019	0,0003	0,0021	0,0002		
PS_16			0,0133	0,0013	0,0135	0,0011	0,0043	0,0001	0,0275	0,0033	0,0034	0,0004	0,0018	0,0004		
PS_17	0,0035	0,0006	0,0023	0,0003	0,0113	0,0012	0,0048	0,0006	0,0245	0,0025	0,0025	0,0001	0,0018	0,0002		
PS_18			0,0111	0,0016	0,0041	0,0009	0,0033	0,0005	0,0361	0,0042	0,0023	0,0001	0,0016	0,0002		
PS_19	0,0124	0,0029	0,0135	0,0033	0,0088	0,0023	0,0032	0,0007	0,0269	0,0066	0,0025	0,0006	0,0019	0,0003		
PS_20	0,0034	0,0005	0,0131	0,0023	0,0044	0,0007	0,003	0,0008	0,0229	0,0043	0,0023	0,0004	0,0016	0,0003		
PS_21	0,0075	0,0012	0,0165	0,0024	0,0095	0,0014	0,0022	0,0004	0,0236	0,0018	0,002	0,0004	0,0019	0,0003	0,0013	0,0019

Appendixes

Sample	Sn (%)	+/-	Sb (%)	+/-	Ta (%)	+/-	W (%)	+/-	Pb (%)	+/-	U (%)	+/-
PS_01											0,001	0,0007
PS_02											0,0009	0,0006
PS_03									0,0105	0,0012	0,0012	0,0008
PS_04											0,0011	0,0008
PS_05	0,0023	0,0033									0,0019	0,0003
PS_06			0,034	0,0094	0,0011	0,0016						
PS_07			0,0092	0,0004							0,0015	0,0002
PS_08	0,003	0,0042	0,0131	0,0005							0,001	0,0007
PS_09												
PS_10	0,0803	0,0095	0,17	0,0176	0,0012	0,0017	0,0008	0,0011	0,0214	0,0005	0,0005	0,0007
PS_11			0,117	0,0068							0,001	0,0007
PS_12											0,002	0,0003
PS_13	0,0024	0,0033	0,0371	0,0029								
PS_14			0,0115	0,0017							0,0005	0,0007
PS_15	0,0021	0,003	0,2017	0,0259					0,0177	0,0126		
PS_16			0,0116	0,0011							0,0005	0,0007
PS_17					0,0032	0,0023					0,0005	0,0007
PS_18											0,0009	0,0007
PS_19			0,1769	0,0373					0,0094	0,0067		
PS_20					0,0012	0,0017					0,0015	0,0003
PS_21			0,012	0,001							0,0005	0,0007

Appendixes

I. XRF Results For The Soil Fraction With a Particle Size Above 2mm

Table 7 - XRF results of samples fraction with a particle size > 2mm, with values in % and +/- representing the standard deviation

Sample	K (%)	+/-	Ca (%)	+/-	Ti (%)	+/-	Cr (%)	+/-	Mn (%)	+/-	Fe (%)	+/-	Co (%)	+/-	Ni (%)	+/-
PS_03					0,4005	0,0222			0,0329	0,0088	6,8585	0,2334				
PS_06	1,4506	0,0269	0,3814	0,0386	0,2416	0,0158	0,015	0,002	0,019	0,0023	4,8227	0,1396				
PS_07					0,2553	0,0308			0,026	0,0085	4,5532	0,3012				
PS_08	0,0664	0,0939			0,1905	0,1276			0,0206	0,0146	2,5423	1,7255				
PS_09					0,3803	0,0352			0,0038	0,0054	4,5299	0,4003				
PS_10	0,9499	0,6722			0,2179	0,0174	0,0034	0,0048	0,0058	0,0042	3,4172	0,07			0,0007	0,0009
PS_11					0,2847	0,1334			0,0194	0,0089	3,0853	1,526				
PS_12					0,4391	0,0595			0,0507	0,0195	3,8544	0,3332	0,0032	0,0045	0,0013	0,0019
PS_13	0,6637	0,4698			0,2489	0,0205	0,0037	0,0052	0,0088	0,0063	3,592	0,1523				
PS_14					0,3067	0,0729			0,1765	0,0535	8,3592	1,2296	0,0029	0,0041		
PS_15	0,7142	0,0627			0,2084	0,0174	0,0083	0,0059	0,0239	0,0066	2,5634	0,0608	0,0033	0,0047	0,0024	0,0008
PS_16	0,3454	0,4885			0,5374	0,0656					5,2309	0,8199				
PS_17	0,0727	0,1028			0,2759	0,0375					3,6326	0,6926				
PS_18					0,3883	0,0388			0,0488	0,0082	7,2467	0,8179				
PS_19					0,2707	0,0323			0,0171	0,0039	5,0872	0,4788				
PS_20					0,3092	0,1283			0,0025	0,0036	4,1749	1,4367				
PS_21					0,2166	0,032			0,0132	0,0023	2,845	0,4253				

Appendixes

Sample	Cu (%)	+/-	Zn (%)	+/-	As (%)	+/-	Rb (%)	+/-	Sr (%)	+/-	Y (%)	+/-	Zr (%)	+/-	Nb (%)	+/-
PS_03	0,0007	0,0011	0,0064	0,0008			0,0081	0,0002	0,0028	0,0001	0,0019	0,0004	0,0133	0,0001	0,0011	0,0008
PS_06	0,001	0,0014	0,0045	0,0004	0,0077	0,0007	0,0098	0,0007	0,0064	0,0003	0,0015	0,0002	0,0131	0,0008	0,002	0,0001
PS_07			0,0054	0,0016	0,004	0,0004	0,0111	0,0012	0,0064	0,0007	0,0019	0,0004	0,0146	0,0018	0,0018	0,0002
PS_08			0,0083	0,0059	0,006	0,0044	0,0088	0,0063	0,0035	0,0025	0,0012	0,0009	0,0092	0,0066	0,0013	0,0009
PS_09			0,013	0,0007	0,0072	0,0014	0,0113	0,0016	0,0057	0,0009	0,0027	0,0003	0,0148	0,0026	0,0018	0,0004
PS_10	0,0004	0,0006	0,01	0,0006	0,0087	0,0004	0,0116	0,0007	0,0064	0,0004	0,0016	0,0001	0,0146	0,0005	0,0017	0,0002
PS_11			0,0062	0,0037	0,0124	0,0089	0,0067	0,0047	0,0042	0,003	0,0019	0,0013	0,012	0,0086	0,0012	0,0008
PS_12	0,0016	0,0023	0,0145	0,0037	0,0057	0,0002	0,0265	0,0018	0,0118	0,0009	0,0034	0,0003	0,034	0,0045	0,0025	0,0004
PS_13	0,0012	0,0008	0,0049	0,0006	0,0038	0,0004	0,0058	0,0003	0,0032	0,0004	0,0015	0,0001	0,0114	0,0008	0,0016	0,0001
PS_14	0,001	0,0015	0,0032	0,0002	0,0042	0,0008	0,0086	0,0016	0,0052	0,0009	0,0026	0,0004	0,0167	0,003	0,0018	0,0004
PS_15	0,0024	0,0005	0,0033	0,0003	0,0449	0,0044	0,0038	0,0001	0,0027	0,0003	0,0013	0,0002	0,0087	0,0004	0,0014	0,0001
PS_16			0,0017	0,0013			0,0097	0,0024	0,0098	0,0023	0,0027	0,0008	0,0166	0,0041	0,0023	0,0005
PS_17	0,0007	0,0009	0,0005	0,0007	0,0018	0,0013	0,0011	0,0008	0,0051	0,0011	0,0023	0,0005	0,0117	0,0028	0,002	0,0003
PS_18	0,0007	0,0009	0,0069	0,0004			0,0138	0,0021	0,0049	0,0009	0,0027	0,0003	0,0161	0,0026	0,002	0,0003
PS_19			0,0059	0,0007	0,0119	0,0011	0,0079	0,0012	0,0043	0,0006	0,0017	0,0001	0,0125	0,0014	0,0015	0,0002
PS_20			0,0027	0,0018	0,004	0,0018	0,0085	0,0034	0,0025	0,0011	0,0019	0,0006	0,0143	0,0056	0,0015	0,0003
PS_21	0,0005	0,0007	0,0046	0,0015	0,0066	0,0012	0,0205	0,0043	0,0084	0,0018	0,001	0,0008	0,0129	0,0032	0,0016	0,0003

Appendixes

Sample	Mo (%)	+/-	Cd (%)	+/-	Sn (%)	+/-	Sb (%)	+/-	Ba (%)	+/-	Ta (%)	+/-	W (%)	+/-	U (%)	+/-
PS_03	0,0008	0,0006													0,0004	0,0006
PS_06	0,0021	0,0003					0,1345	0,0195								
PS_07	0,0018	0,0005					0,0056	0,004							0,0004	0,0005
PS_08	0,001	0,0007													0,0004	0,0006
PS_09	0,0016	0,0004													0,0005	0,0007
PS_10	0,0022	0,0001	0,0013	0,0019	0,0093	0,0021	0,0798	0,0026							0,0005	0,0007
PS_11	0,0011	0,0008					0,3264	0,224	0,022	0,0311						
PS_12	0,0012	0,0009					0,0025	0,0035			0,0015	0,0021			0,0015	0,0001
PS_13	0,0019	0,0003					0,0052	0,0038			0,0009	0,0013			0,0005	0,0007
PS_14	0,0017	0,0004	0,0027	0,002												
PS_15	0,0024	0,0001					0,0637	0,0043			0,0034	0,0001	0,0012	0,0009	0,0009	0,0006
PS_16	0,0011	0,0008			0,0019	0,0027	0,0124	0,0035			0,0015	0,0022			0,0004	0,0006
PS_17	0,002	0,0004									0,0025	0,0019			0,0004	0,0006
PS_18	0,0016	0,0003			0,0023	0,0033	0,0034	0,0048							0,0009	0,0007
PS_19	0,0009	0,0006	0,0013	0,0019			0,038	0,0051							0,0004	0,0005
PS_20	0,001	0,0007													0,0006	0,0008
PS_21	0,0016	0,0004									0,0017	0,0024			0,0009	0,0007

II. Total Organic Carbon Results

Table 8 – Experimental results for the determination of total organic carbon.

Sample	Soil mass (g)	Volume of ferrous ammonium sulphate (mL)	Sample	Organic Carbon (%)
B1		20,1		
B2		19,9		
1	0,56	15,8	PS_01	1,5%
2	0,52	14	PS_02	2,3%
3	0,51	11,9	PS_03	3,1%
4	0,54	10,3	PS_04	3,5%
5	0,53	7,4	PS_05	4,6%
6	0,51	11,1	PS_06	3,4%
7	0,5	14,8	PS_07	2,0%
8	0,51	14,1	PS_08	2,3%
B5		19,8		
B6		20,1		
9	0,52	12,7	PS_09	2,7%
10	0,52	13,5	PS_10	2,4%
11	0,54	8	PS_11	4,3%
12	0,68	2,4	PS_12	5,0%

Appendixes

Sample	Soil mass (g)	Volume of ferrous ammonium sulphate (mL)	Sample	Organic Carbon (%)
B8		19,9		
B9		19,9		
13	0,56	12,9	PS_13	2,4%
14	0,52	13,6	PS_14	2,4%
15	0,53	12,3	PS_15	2,8%
16	0,54	16,8	PS_16	1,1%
17	0,53	18	PS_17	0,7%
18	0,58	11,8	PS_18	2,7%
19	0,5	12	PS_19	3,1%
20	0,52	17,5	PS_20	0,9%
21	0,53	14	PS_21	2,2%

III. Soil pH

Table 9 - Soil pH

Sample	Soil Mass (g)	pH
PS_01	20,3	5,494
PS_02	20,75	5,473
PS_03	20,02	5,488
PS_04	20,35	5,557
PS_05	20,25	5,316
PS_06	20,45	7,07
PS_07	20,1	6,649
PS_08	20,48	6,461
PS_09	20,11	5,82
PS_10	20,13	7,027
PS_11	20,34	6,748
PS_12	20,03	5,184
PS_13	20,05	5,261
PS_14	20,46	4,715
PS_15	20,15	5,466
PS_16	20,77	4,967
PS_17	20,22	4,93
PS_18	20,58	5,672
PS_19	20,69	6,601
PS_20	20,6	5,294
PS_21	20,57	7,318

Net Acid Generation (NAG) Results For The Soil Fraction With a Particle Size Below 2mm

Table 10 - NAG of samples fraction with a particle size < 2 mm

Sample	Ps_01	Ps_02	Ps_03	Ps_04	Ps_05	Ps_06	Ps_07	Ps_08	Ps_09	Ps_10	Ps_11	Ps_12	Ps_13	Ps_14	Ps_15	Ps_16	Ps_17
Weight (g)	2,62	2,51	2,5	2,51	2,59	2,5	2,51	2,51	2,51	2,58	2,57	2,61	2,55	2,63	2,58	2,52	2,51
Oxidation Time	20h	20h	20h	20h	22h	13h	13h	13h	13h	13h	15h45	15h45	15h45	15h45	22h	22h	22h
Boiling Time	2h	2h	2h	2h	2h	2h	2h	2h	2h	2h	2h	2h	2h	2h	2h	2h	2h
NAG_pH (Before Titration)	7,515	7,75	7,493	7,516	8,201	8,438	8,063	7,913	7,614	8,068	7,831	7,789	4,584	4,733	3,568	3,622	3,719
V_{NaOH} (mL)															2,6	1,3	1
V_{NaOH} (mL)													4	3,8	9	5,4	5,5
NAG 4.5 (kg H2SO4/t)	**0**	0	0	0	0	0	0	0	0	0	0	0	0	0	4,937	2,527	1,952
NAG pH 7 (kg H2SO4/t)	**0**	0	0	0	0	0	0	0	0	0	0	0	**7,7**	**7,1**	**17,1**	**10,5**	**10,7**

Sample	Ps_10	Ps_11	Ps_12	Ps_13	Ps_14	Ps_15	Ps_16	Ps_17	Ps_18	Ps_19	Ps_20	Ps_21
Weight (g)	2,58	2,57	2,61	2,55	2,63	2,58	2,52	2,51	2,53	2,51	2,54	2,59
Oxidation Time	13h	15h45	15h45	15h45	15h45	22h	22h	22h	24h	24h	24h	24h
Boiling Time	2h	2h	2h	2h	2h	2h	2h	2h	2h	2h	2h	2h
NAG_pH (Before Titration)	8,068	7,831	7,789	4,584	4,733	3,568	3,622	3,719	6,795	7,381	4,558	7,101
V_{NaOH} (mL)						2,6	1,3	1				
V_{NaOH} (mL)				4	3,8	9	5,4	5,5	0,3		2,8	
NAG 4.5 (kg H2SO4/t)	0	0	0	0	0	4,937	2,527	1,952	0	0	0	0
NAG pH 7 (kg H2SO4/t)	0	0	0	**7,7**	**7,1**	**17,1**	**10,5**	**10,7**	**0,6**	**0**	**5,4**	**0**

IV. Net Acid Generation (NAG) Results For The Soil Fraction With a Particle Size Above 2 mm

Table 11 - NAG of samples fraction with a particle size > 2 mm

Sample	Ps_01	Ps_02	Ps_03	Ps_04	Ps_05	Ps_06	Ps_07	Ps_08	Ps_09	Ps_10	Ps_11
Weight (g)			2,58			2,56	2,51	2,78	2,57	2,61	2,51
Oxidation Time			13h30			13h30	16	14h30	13h30	13h30	14h30
Boiling Time			2h			2h	2	2h	2h	2h	2h
NAG_pH (Before Titration)			5,934			8,388	7,372	6,563	5,507	6,352	2,766
V_{NaOH} (mL)											2,7
V_{NaOH} (mL)			0,9					0,5	1,5	0,6	6,7

Sample	Ps_12	Ps_13	Ps_14	Ps_15	Ps_16	Ps_17	Ps_18	Ps_19	Ps_20	Ps_21
Weight (g)	2,63	2,61	2,53	2,56	2,58	2,66	2,64	2,59	2,6	2,55
Oxidation Time	15h30	14h30	14h30	16h30	15h30	15h30	15h30	16h30	16h30	16h30
Boiling Time	2h	2h	2h	2h	2h	2h	2h	2h	2h	2h
NAG_pH (Before Titration)	7,898	5,6	6,792	6,084	5,234	5,431	6,839	9,093	5,777	3,884
V_{NaOH} (mL)										0,4
V_{NaOH} (mL)		1,6	0,2	1	1,3	1,5	0,2		1,1	1,2

Appendixes

V. Reference Values for Soils from APA

Table 12 - Reference values for heavy metals from APA

TABLE B – Reference values for soils within 30 meters of a surface water body					
CE Number	CAS	Contaminant	Reference Values (mg/kg dry)		
			Use of underground water		No use of underground water
			Agricultural use	Urban /Industrial /Comercial use	Urban /Industrial /Comercial use
231-146-5	7440-36-0	Antimony	1	1,3	1,3
231-148-6	7440-38-2	Arsenic	11	18	18
231-152-8	7440-43-9	Cadmium	1	1,2	1,2
231-100-4	7439-92-1	Lead	45	120	120
231-159-6	7440-50-8	Copper	62	92	92
231-111-4	7440-02-0	Nickel	37	82	82
231-175-3	7440-66-6	Zinc	290	290	290